ELECTRONICS AND SPACE DIVISION

EMERSON

NASA CR 66679

Report No. 3001-3

COMPILATION OF ROCKET SPIN DATA

FINAL REPORT, VOLUME III
DATA EVALUATION
AND RECOMMENDATIONS

Prepared for:

NASA LANGLEY RESEARCH CENTER
LANGLEY STATION
HAMPTON, VIRGINIA

CONTRACT NO. NAS1-6833

23 August 1968

NASA CR 66679

FINAL REPORT

COMPILATION OF ROCKET SPIN DATA

VOLUME III: DATA EVALUATION AND RECOMMENDATIONS

by

Leo J. Manda, Emerson Electric Co.

Prepared under Contract No. NAS1-6833
for NASA Langley Research Center

PREFACE

Under Contract No. NAS1-6833 with the NASA Langley Research Center, the Emerson Electric Company has conducted a program to compile and evaluate all available data relating to the effects of (spin) acceleration on solid propellant rocket motor performance. This compilation of Rocket Spin Data (CRSD) program was initiated in November 1966 and completed in August 1968.

The CRSD program was directed by Mr. Leo J. Manda of Emerson Electric, with assistance from Mr. John E. Mosier, particularly with the computer programs generated during the course of this study. The program effort was monitored by Mr. Melvin H. Lucy of NASA Langley, who also provided a great deal of assistance with the data acquisition effort.

ABSTRACT

Test data compiled and analyzed during the Compilation of Rocket Spin Data program indicates that practically every propellant formulation variable and motor operating condition will influence the sensitivity of a composite solid propellant to a spin environment. The increase in burn rate noted with spin is shown to be a function of motor size, spin rate, grain configuration, and operating pressure; and also of aluminum (Al) particle size, ammonium perchlorate (AP) particle size, and type of binder. With qualitative data currently available regarding the effects of changes in Al or AP particle size, a research program to quantify the effects of different binders is recommended for immediate implementation. Additional recommendations include an analytical/experimental program to better define the effects of spin on motor gas dynamics and the usual reductions in nozzle efflux capability and gross deviations in end-burning motor performance attributed to the spinning gas flow.

SECTION I

INTRODUCTION

For a number of years, the NASA and other Government agencies have been instrumental in developing solid propellant rocket motors which are spun to provide dynamic stability or to reduce dispersion due to thrust misalignment. Prior to the use of metal additives in these propellants, no serious problems attributed to the spin environment had been encountered in vehicles of interest to the NASA, although definite spin sensitivity had been noted in a number of spin-stabilized tactical rocket motors. However, with the use of aluminum and other metal additives in the more recent propellant formulations, various motor performance anomalies have been experienced with motors subjected to even low spin rates.

Recognizing that a considerable amount of data pertinent to the effects of spin on solid propellant motor performance has been generated by Government agencies and contractors, the NASA Langley Research Center has contracted the Emerson Electric Co. to compile and evaluate this data in order to provide: (1) an improved basis for dealing with the problems associated with motors operating in this environment; and (2) guidance for future research efforts in this area.

The results of this Compilation of Rocket Spin Data (CRSD) program are presented in this and two additional volumes of the CRSD final report. These volumes are organized according to:

Volume I - Acceleration Test Facilities: describes the various spin and centrifuge test facilities available for testing solid propellant rocket motors in acceleration environments.

Volume II - Literature Survey: summarizes the results of the extensive CRSD literature survey, documenting the acceleration effects experienced in various motor development programs and specifying the current state of the art in acceleration studies.

Volume III - Data Evaluation and Recommendations: examines the test data obtained from the various Government agencies and contractors and recommends promising areas for future research activities.

This third volume of the CRSD final report discusses the methods used to acquire and analyze the acceleration test data accumulated during the CRSD program, and presents detailed analyses of some of the more closely controlled test data. Along with the results of the literature survey, the results of these analyses form the bases of recommended future research activities devoted to the study of acceleration phenomena.

SECTION II

DATA ACQUISITION

In an attempt to obtain a maximum amount of meaningful data for use in evaluating the effects of spin on solid propellant motor performance, the CRSD data acquisition effort was initially intended to be conducted in two phases. The first phase involved generating an acceleration data questionnaire for submittal to all known current or recent investigators of acceleration phenomena. The second phase involved personal interviews with the respondents to this questionnaire to discuss their particular areas of endeavor.

The acceleration data questionnaire is enclosed herewith as Appendix A. As indicated, this questionnaire is divided into four basic sections:

1 - Reference Sources: requests a bibliography of reference material dealing with propellant, combustion, or exhaust gas behavior in acceleration fields, other than the references enumerated in (1)*.

2 - Analytical Studies: requests a summary of the results of any in-house or contracted analytical studies of combustion or nozzle expansion phenomena associated with acceleration environments.

3 - Test Facilities: requests a definitive description of both spin and centrifuge test facilities constructed for acceleration testing.

4 - Motor Performance: requests detailed information on the motors and propellants tested during in-house or contracted studies of acceleration phenomena, or with which acceleration effects were found to be significant during (flight) test. This detailed motor performance data was intended to form the bases for the overall data correlation effort to be accomplished as part of the CRSD program.

In February 1967, this questionnaire was submitted to the 33 potential data sources listed in Appendix B. As indicated in (2) - (5), practically no useful motor performance data was obtained from the responses received. However, this effort was most successful in identifying previously unknown reference sources and acceleration test facilities.

---

*Numbers in parentheses refer to references included in Section VI of this report.

Failing to acquire any meaningful performance data, the original intention of using the personal interviews to discuss individual test results (and their relation to similar data generated by other sources) was altered to using these personal contacts primarily to acquire test data. However, this effort also proved generally unsuccessful.

In general, most organizations which had been active in spin test work indicated that the lack of funds and/or available manpower to compile and organize the data had precluded their participation in this data acquisition effort. Unfortunately, this situation is symptomatic of a general lack of test documentation to any extent other than the minimum acceptable. One organization indicated that, although more than 1000 spin test firings of various motors had been accomplished, little if any of the data acquired would be acceptable for attempting an analysis of the test results to quantify the effects of the spin environments on motor performance. Moreover, a number of the tests had been performed on simply a go/no-go basis.

When dealing with phenomena (such as spin effects) which are not generally understood, good engineering practice would seem to demand that all test firings be documented as fully as possible, with an eye toward the possibility that an eventual analytic evaluation of the test results might lead to an improved understanding of the phenomena involved. Unfortunately, this procedure has not been followed in most motor development programs, thereby rendering the data acquired therefrom practically useless for quantitative evaluation.

With the lack of suitable data from the majority of the motor development programs, the non-developmental research studies have been the major sources of the data analyzed herein. Such studies have been conducted primarily by the NASA Langley Research Center (LRC), the U.S. Naval Postgraduate School (NPS), and United Technology Center (UTC).

SECTION III

METHODS OF ANALYSIS

During the course of the CRSD program, two digital computer programs were generated to compile, collate, and analyze the test data acquired. The COMSORT program is designed to compile and collate this data according to specified constraints. The DRN program is designed to analyze individual pressure and/or thrust histories to obtain motor performance parameters, and to compare these results with two different methods of determining burn rate augmentation in acceleration fields.

COMSORT Computer Program

The COMSORT (compile/sort) computer program is an integrated series of three sub-programs developed to compile and collate the results of the approximately 750 acceleration tests accumulated during the CRSD data acquisition effort. This program was developed for the Emerson Electric Co.'s Honeywell 200 digital computer system.

The three COMSORT sub-programs are specifically directed to: (A) read the input data from punched cards and reproduce it on magnetic tape in the output format; (B) collate this random data in a sequentially ordered data file according to one major parameter and up to nine minor parameters; and (C) screen the data subject to as many as eight specified constraints, counting the number of cases satisfying each constraint, and selectively print out the results. As described in detail in (6), programs (A) and (C) are written in FORTRAN, and program (B) in assembly (binary) language. A detailed flow chart of the composite program is presented in Figure 3-1.

The data accumulated from the majority of the motor development tests and research studies discussed in (7) was compiled in (6). However, because of the generally poor test documentation, frequent lack of reference values, and the fact that potentially significant factors affecting motor performance were frequently altered considerably during a development effort in order to "fix" an improperly functioning motor, this method of data analysis was found to be unsatisfactory for developing any quantitative estimate of the effects of a spin environment on motor performance. Thus the development of the DRN computer program was initiated to allow performing more detailed analyses of individual test results obtained from the more closely controlled research studies.

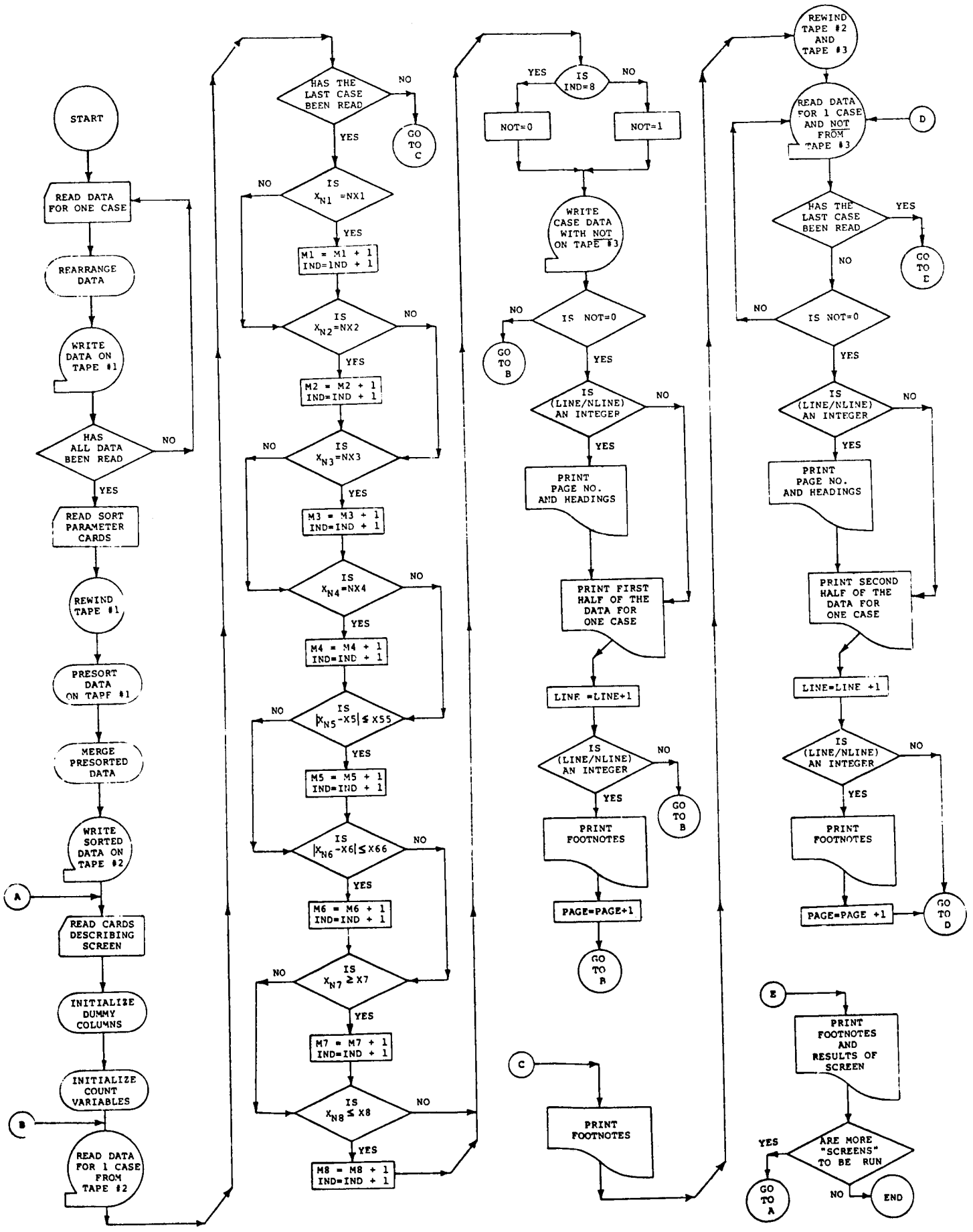

FIGURE 3-1: COMSORT Program Flow Chart

DRN Computer Program

In addition to accomplishing the usual objectives of integrating and averaging pressure and thrust histories, the DRN (Data Reduction and Normalization) computer program uses the data thus obtained to compare measured motor performance with that predicted by two different methods of estimating burn rate augmentation in an acceleration environment. Written in FORTRAN, this program was developed for use with the CDC 6400 digital computer system.

Methods of Analysis

Two different methods of determining burn rate augmentation are employed in the DRN computer program.

Method [A] assumes that the augmented burn rate (r_A) at a given acceleration level can be described by:

$$[1] \qquad r_A = (AF) r_t = (AF) r_x \ (P/P_x)^n$$

where r_t is the theoretical burn rate at the measured combustion pressure (P), obtained from static (non-accelerating) burn rate data where r_x is the (base) burn rate at the reference pressure (P_x) and n is the pressure exponent (assumed constant with acceleration level). The burn rate augmentation factor (AF) is assumed constant with both pressure and time, and is determined by requiring that this factor times the theoretical web consumed (W_t) over burn time (t_B) be equal to the measured propellant web thickness (W). Thus the augmentation factor is determined from:

$$[2] \qquad (AF) = W/W_t = W/\int_0^{t_B} r_x (P/P_x)^n dt$$

Assuming that the propellant density (ρ) and grain surface areas (S) normal (S_r) and parallel (S_e) to the acceleration vector are known as functions of the web thickness (W_r), method [B] calculates the instantaneous augmented burning rate (r_r) as that required to yield the measured value of combustion pressure. Thus values of r_r are calculated without reference to any predetermined burn rate/pressure relationship, according to:

$$[3] \qquad r_r = (\dot{m}_o - \dot{m}_e)/\rho \, S_r$$

where $\dot{m}_o = C_D P A_*$ is the total nozzle efflux
and $\dot{m}_e = \rho r_t S_e$ is the mass generated by the (end) surfaces of the grain parallel to the acceleration vector, which are assumed to be unaffected by the acceleration environment. ($S_e = 0$ for neutral-burning grain geometries.)

While method [A] assumes that the burn rate augmentation factor is constant over the burning interval, method [B] yields instantaneous values of burn rate augmentation factor $(AF)_i$, given by:

$$[4] \qquad (AF)_i = r_r/r_t$$

Thus an average burn rate augmentation ($\overline{AF}$) could be calculated for method [B] from:

$$[5] \qquad (\overline{AF}) = (1/t_B)\int_0^{t_B} (r_r/r_t)dt$$

The basic DRN program logic is outlined in Figure 3-2. As indicated, either neutral-burning or cylindrically perforated grains (with 0, 1, or 2 ends burning) can be analyzed. Although a complete description of the DRN program is included herein as Appendix C, some of the salient features of the analytical techniques employed are outlined below.

Nozzle Throat Area (A_*)

If the nozzle throat is found to erode during a motor firing, this erosion must be accounted for in determining nozzle efflux. Therefore, based upon the usual transient nature of the heating process, variations in A_* are assumed exponential rather than linear. Thus the instantaneous nozzle throat area is given by:

$$[6] \qquad A_* = A_{*i} + (A_{*f}-A_{*i})(t/t_f)\ \exp\ (t/t_f-1)$$

where A_{*i} is the pre-test area and A_{*f} is the post-test area, assumed to occur at final time (t_f). From [6] the average throat area ($\overline{A}_*$) is given by:

$$[7] \qquad \overline{A}_* = A_{*i} + (A_{*f}-A_{*i})/e$$

Figure 3-3 gives a sample variation in A_* for a 10% overall increase in throat area.

Mass Flow Coefficient (C_D)

From the conservation of mass, the nozzle efflux ($\dot{m}_o$) integrated over total action time (t_f) must be equal to the mass of propellant expended (m). Therefore, actual values of C_D are calculated for each test from:

$$[8] \qquad C_D = m/\int_0^{t_f} PA_*dt$$

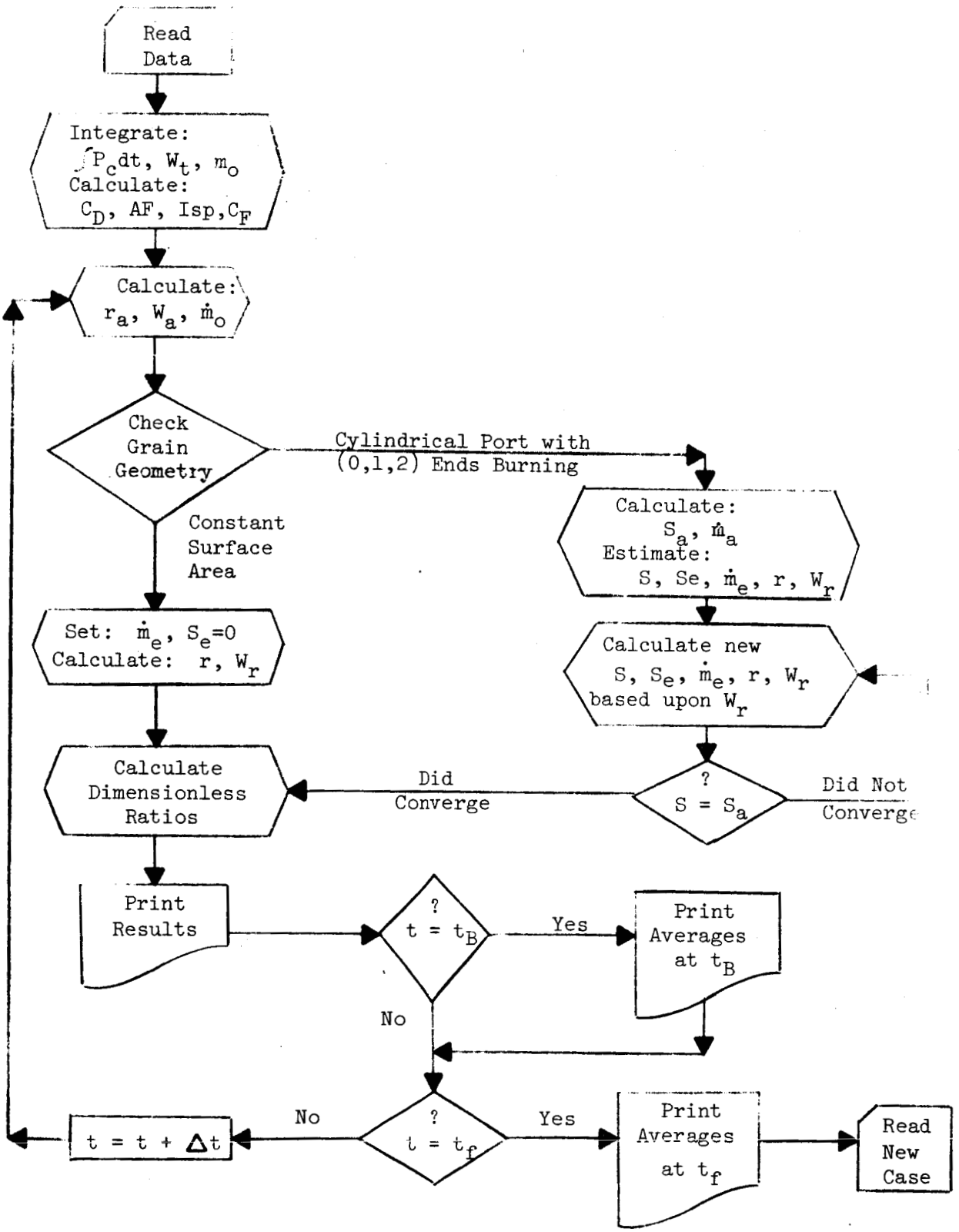

FIGURE 3-2: DRN Program Flow Chart

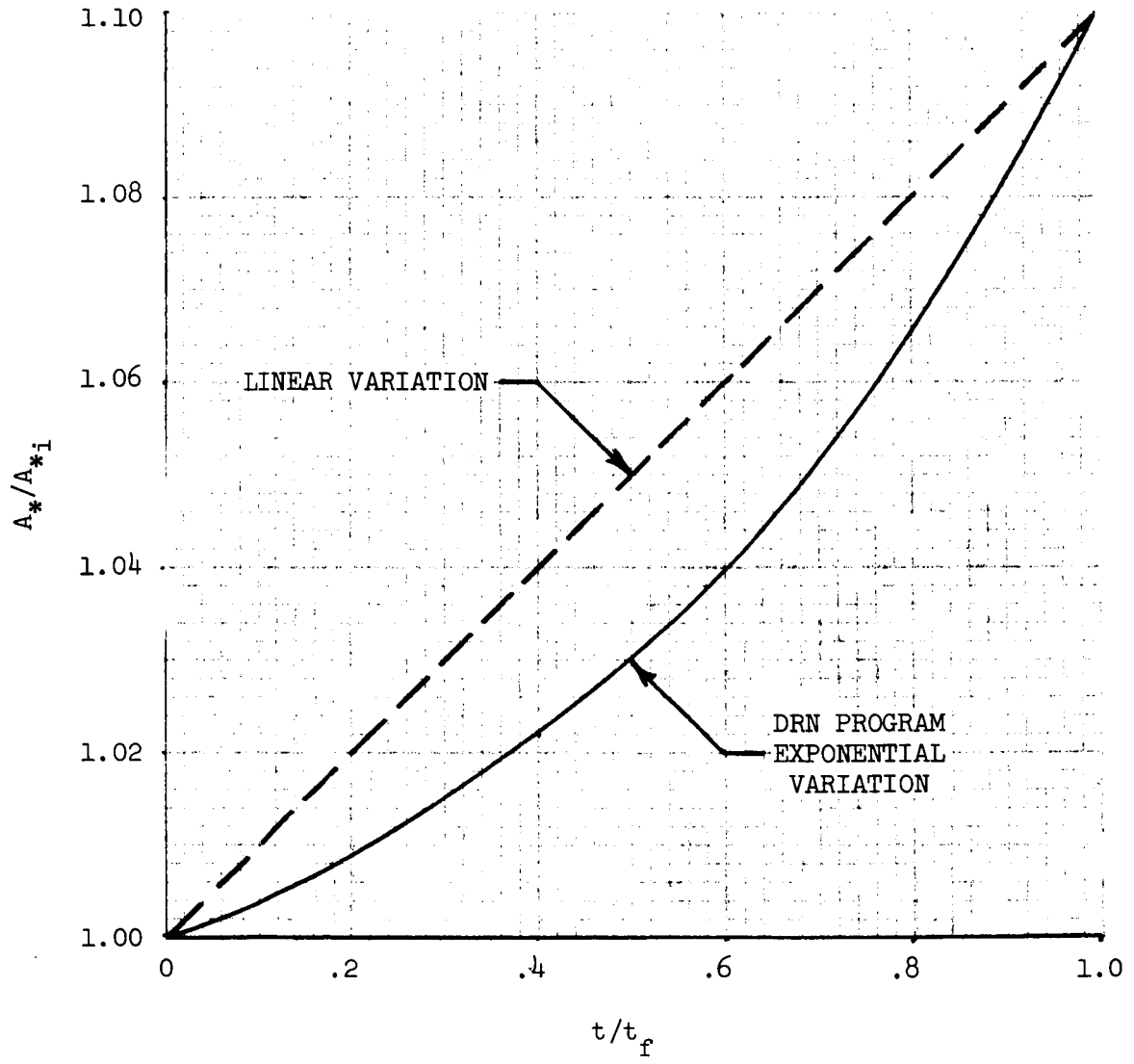

FIGURE 3-3: Variation in Nozzle Throat Area

Since all data points are read in simultaneously and stored in matrix form, this calculation for C_D is performed at the outset of the calculation sequence, and actual values of C_D are used for all subsequent motor performance calculations.

Integration Procedures

Assuming linear pressure variations between data input points, the trapezoidal rule is used for determining all integrals except for the values of web consumed calculated for method [A]. As developed in (8), the web consumed (ΔW) during any time interval (t_2-t_1) over which the pressure varies linearly from P_1 to P_2 (and $P_2 \neq P_1$) is given exactly by:

$$[9A] \qquad \Delta W_a = (P_2 r_2 - P_1 r_1)(t_2-t_1)/(n+1)(P_2-P_1)$$

where r is the burning rate (r_A) calculated from [1]. If $P_2 = P_1$, ΔW_a is given simply by:

$$[9B] \qquad \Delta W_a = r_1(t_2-t_1)$$

With no specific burning rate law assumed in method [B], changes in web thickness are determined using the trapozoidal integration method.

SECTION IV

DATA ANALYSIS

In an effort to fully evaluate the state of the art in understanding the effects of spin on solid propellant motor performance, the test results obtained from a number of the more closely controlled investigations of spin phenomena were analyzed in detail. The results of these analyses for selected examples of both end-burning and internal-burning grains operating in spin environments are presented below.

MICOM Spin Tests

Perhaps the least understood of all spin phenomena is that associated with the severe centerline coning of end-burning grains equipped with a single converging/diverging nozzle. As discussed in (7), this phenomenon has been observed by investigators at Picatinny Arsenal, the Naval Weapons Center, and the U.S. Army Missile Command (MICOM) at Redstone Arsenal, among others.

As reported in (9), spin tests of a 40mm-diameter end-burning grain of non-aluminized polyvinyl chloride composite propellant yielded severe overpressurization of the motor, resulting in nozzle ejection and grain extinguishment. The two partially burned grains recovered from these tests were both found to exhibit the usual centerline coning, with the depth of the "cone" increasing with spin rate. The burning surface profiles scaled from photographs of these extinguished grain sections have been used as boundary conditions for a computer simulation of motor performance.

As indicated in Figure 4-1, the static-test pressure history obtained with this motor is considerably more progressive than would be anticipated for an end-burning grain. Although the cause of this progressivity has not been precisely determined, it has been attributed to a large initial heat loss resulting from the excessive chamber surface area and heat sink capability of the MICOM heavywall test motor. For the computer simulation, a time-varying mass flow coefficient (C_D) was used to duplicate the test results. This same variable C_D was also employed in the two subsequent spin-test simulations.

The increased operating pressures experienced with end-burning propellant grains under spin result from both the increased burning rate of the propellant along the grain centerline and from the reduced nozzle efflux capability. Prior to the recovery of these extinguished grains, there was no way to estimate the increased burning rate with any degree of certainty. However, with these samples, it was possible to force the simulated grain surface regression to match the extinguished burning surface profiles. As indicated in

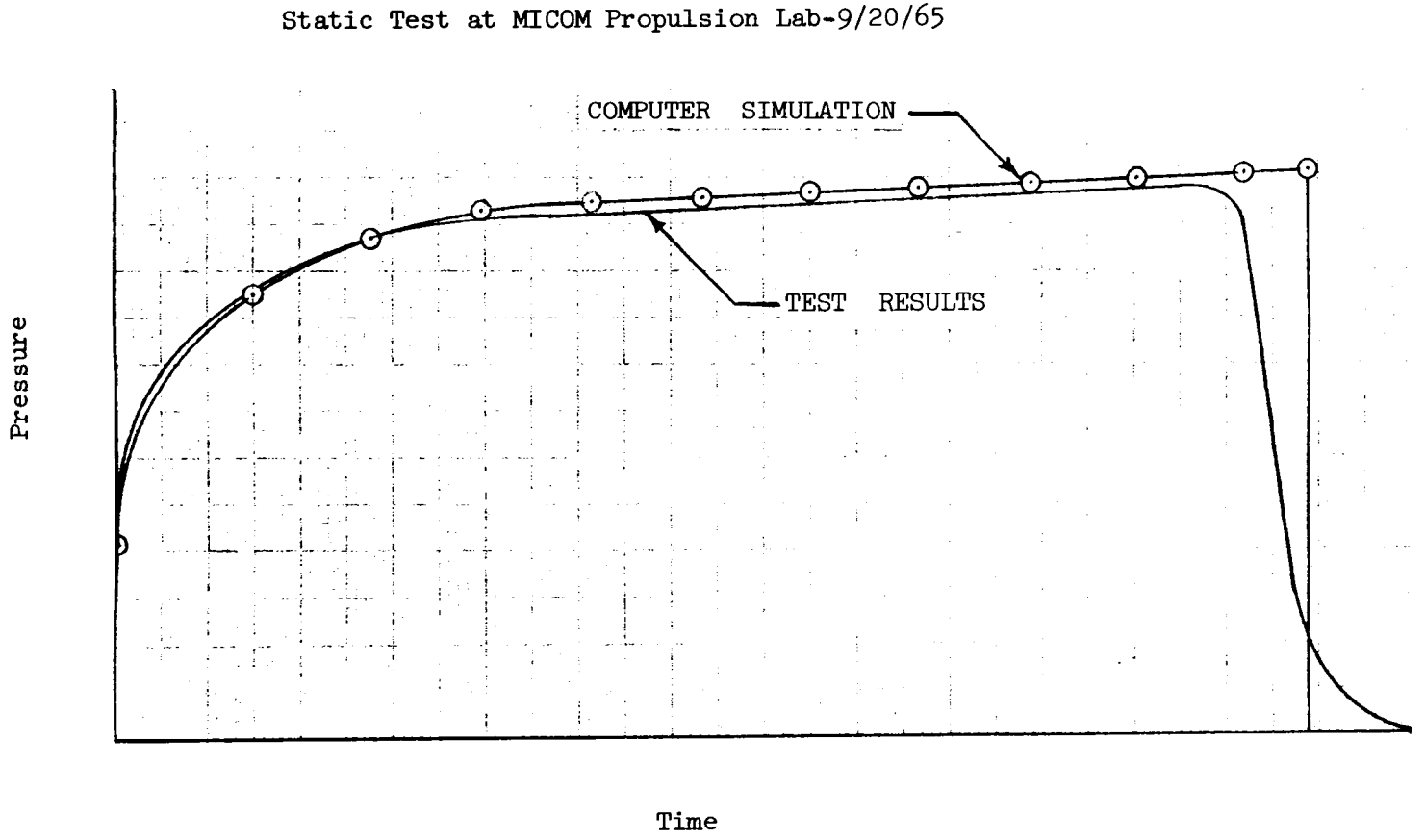

FIGURE 4-1: Comparison of Computer Simulation with Static Test Data

Figures 4-2 and 4-3, these profiles were matched to a high degree of accuracy by assuming that the base burn rate under spin (r_{xs}) varies according to:

[10] $$r_{xs}(R) = (r_x)\{1 + .5K_1[1 + \cos(\pi R/2)]\} \text{ for } R < K_2$$

and

[11] $$r_{xs}(R) = r_x \text{ for } R \geq K_2$$

where R is the radial distance from the grain centerline, r_x is the (static) base burn rate at the reference pressure P_x, and K_1 and K_2 are constants determined from the extinguished grain profiles.

With [10] and [11], combustion pressures (P) were calculated from:

[12] $$(P/P_x)^{1-n} = (\rho/C_D P_x A_*) \oint r_{xs}(R)\, dS$$

where the computed burning rate is integrated over the burning surface (S).

Pressure histories calculated for the one-dimensional nozzle flow implied in [12] are presented in Figures 4-4 and 4-5 for spin rates of 9840 RPM and 12,420 RPM, respectively. As indicated, the measured burning progressivity has not been duplicated.

As discussed in (7), both the combustion process and nozzle efflux capability are influenced by a spin environment. Therefore, in order to determine the effects of nozzle efflux on the performance of this motor, the analytic methods of predicting this phenomenon developed in (10) for rotational flow and (11) for irrotational flow were incorporated in the computer simulation by modifying the (nozzle) mass flow coefficient (C_D) according to:

[13] $$C_{DS} = C_D(\dot{m}_s/\dot{m})$$

where C_{DS} is the mass flow coefficient under spin and $(\dot{m}_s/\dot{m})$ is the reduction in nozzle efflux capability calculated from (10) or (11).

Since the flow emanating from the surface of an end-burning grain is rotational, the analytical method proposed in (11) for irrotational flow should not be applicable to this grain geometry. However, these results were included herein simply for the purpose of comparison.

As indicated in Figures 4-4 and 4-5, none of the analytical attempts to predict the spin-test pressure histories were successful, even when the propellant mass generation history was "known" through the computer simulations of the grain regression profiles. Assuming the validity of the experimental pressure measurements, these results

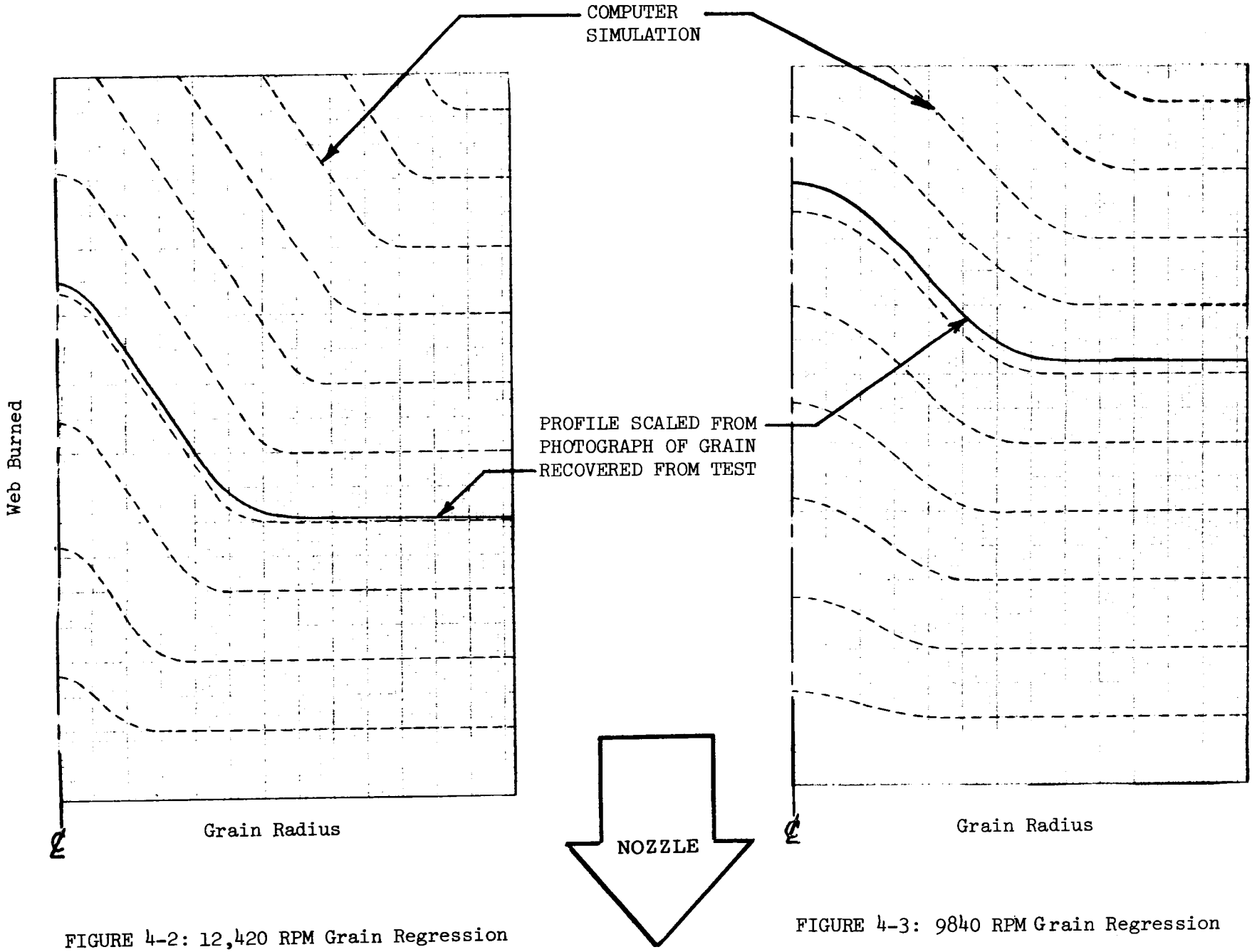

FIGURE 4-2: 12,420 RPM Grain Regression

FIGURE 4-3: 9840 RPM Grain Regression

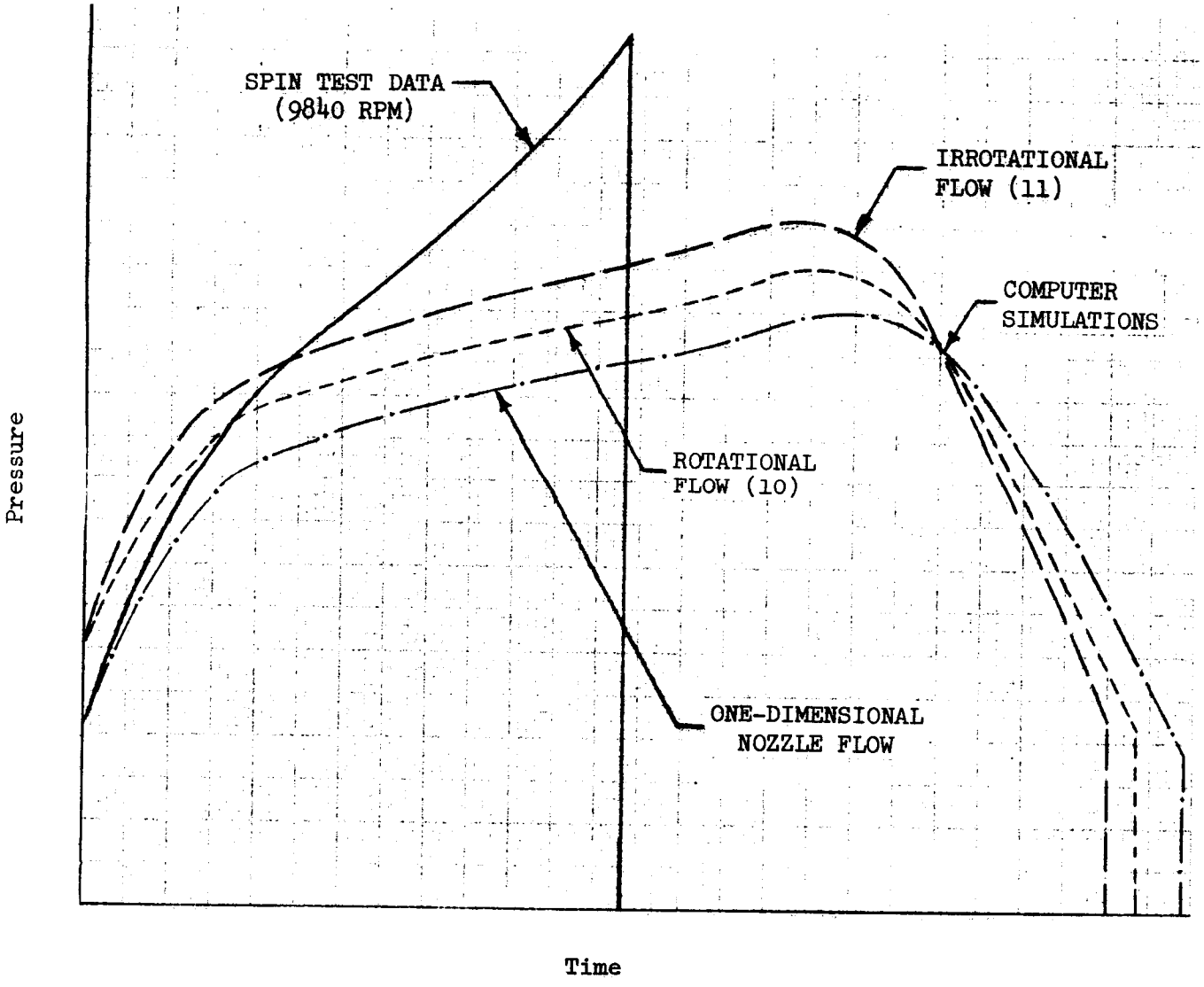

FIGURE 4-4: Computer Simulations of 9840 RPM Pressure History

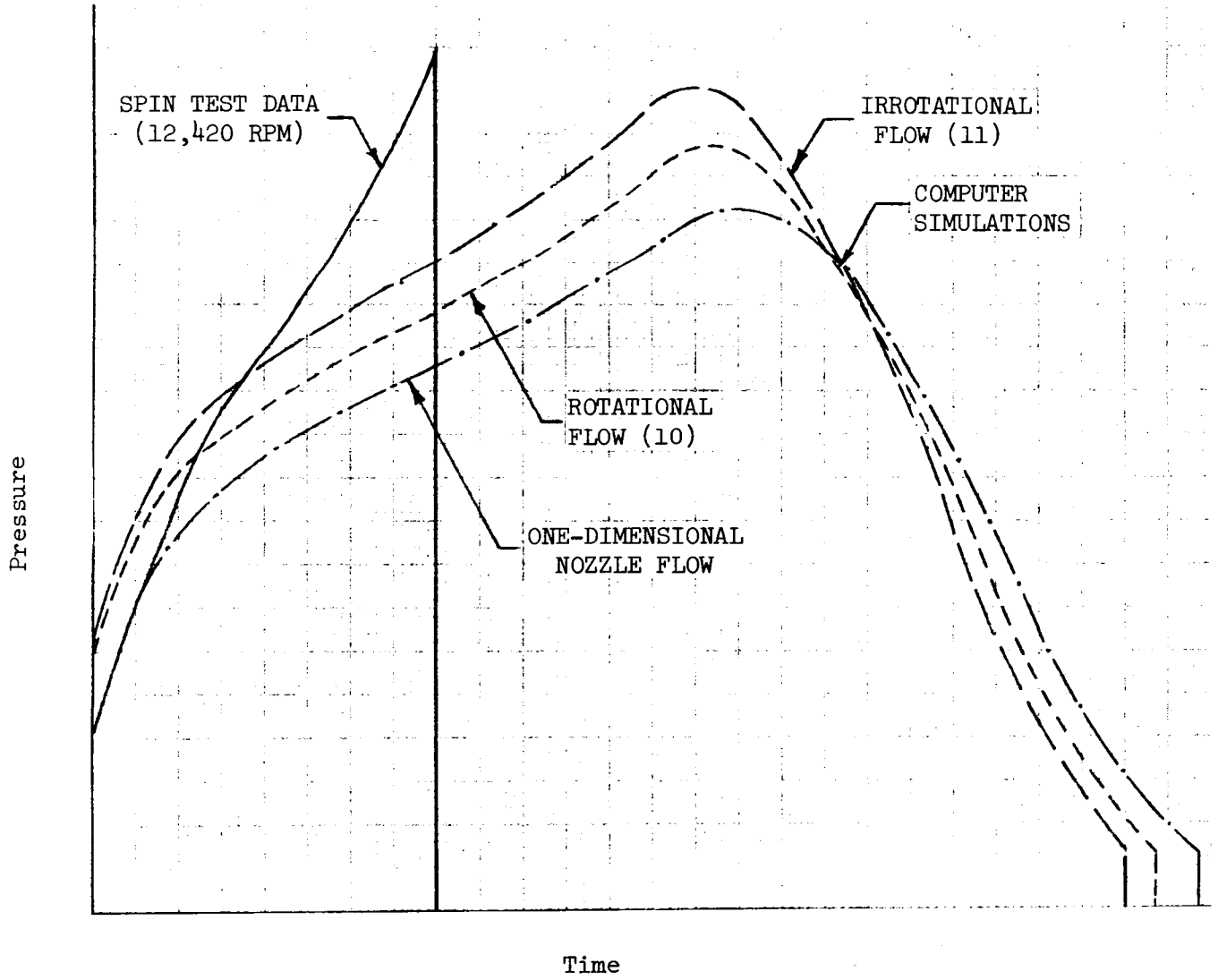

FIGURE 4-5: Computer Simulations of 12,420 RPM Pressure History

and those of other investigators of end-burning grains noted in (7) indicate that nozzle efflux capability appears to be strongly time-dependent. However, the cause of this apparently severe reduction in nozzle efflux has not as yet been determined, although it is assumed to be associated with the as yet undefined gas dynamic mechanism(s) whereby apparently highly erosive (tangential) gas velocities are developed at the grain face near the motor centerline.

UTC Spin Tests

In 1965, the first of a series of three Navy-sponsored spin study programs was initiated at United Technology Center. As reported in (12), (13), (14), and the applicable quarterly progress reports, one of the primary objectives of these programs was to examine the effects of a spin environment on the performance of a basic PBAN propellant formulation and various modifications thereof.

Propellant Formulations

For the purposes of this discussion, the propellants tested by UTC are designated as:

(A) 16.0% PBAN binder
16.0% (46-micron) aluminum (Al)
23.8% (9-micron) ammonium perchlorate (AP)
44.2% (400-micron) AP

(B) 16.0% PBAN
16.0% (8-micron) Al
23.8% (9-micron) AP
44.2% (400-micron) AP

(C) 16.0% PBAN
16.0% (46-micron) dichromated Al
23.8% (9-micron) AP
44.2% (400-micron) AP

(D) 16.0% PBAN
16.0% (46-micron) Al
40.8% (9-micron) AP
27.2% (190-micron) AP

(E) 16.0% PBAN
16.0% (46-micron) Al
23.0% (9-micron) AP
44.0% (190-micron) AP
1.0% Fe_2O_3 burn rate catalyst

(F) 16.0% CTPB (carboxy-terminated polyisobutylene) binder
16.0% (46-micron) Al
23.8% (9-micron) AP
44.2% (400-micron) AP

(G) 19.1% PBAN
28.3% (9-micron) AP
52.6% (400-micron) AP

Propellant (A) is termed the "control" propellant in the UTC reports of the results achieved during this study.

Assuming that the static burning rates (r_t) of these formulations are given by:

[14] $$r_t = r_x(P/Px)^n$$

the base burn rates (r_x) and pressure exponents (n) at a reference pressure (P_x) of 1000 PSIA are given below.

Propellant	Base Rate	Exponent
(A)	.24	.21
(B)	.28	.21
(C)	.288	.31
(D)	.38	.23
(E)	.43	.236
(F)	.172	.18
(G)	.27	.34

Motor Configuration

As illustrated in Figure 4-6, the basic UTC motor uses a cylindrical grain with inhibited end surfaces tapered to provide a theoretical surface progressivity of less than 0.2%. With the 0.607 IN propellant web thickness, the centrifugal acceleration at the propellant surface increases 36.8% over the burning interval with a constant spin rate.

Using Mager's analysis (11) to estimate the effects of motor geometry on nozzle efflux in the spin environment, it can be shown that less than a 5% reduction in efflux capability is anticipated at the maximum acceleration levels achieved during this test series. Thus this effect has been neglected in the analysis and interpretation of the results.

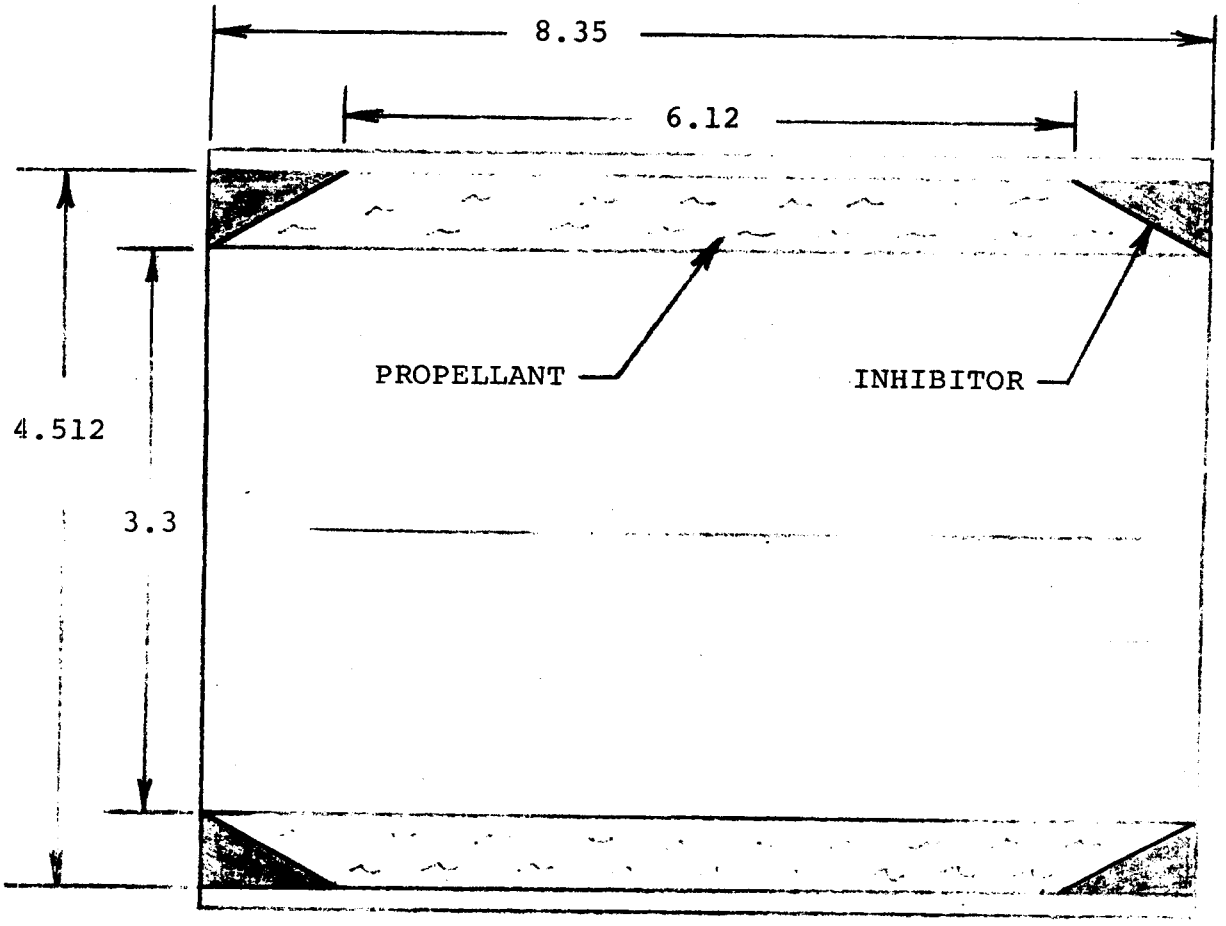

FIGURE 4-6: UTC Test Motor Grain Configuration

Test Results

The test results reported herein include those obtained in nine (9) different series of UTC spin tests. Of these, four series were performed with propellant (A) at different design pressure levels:

Test Series	UTC Design Pressure	Theoretical Avg. Press.	Avg. Press. at 1.0 G	Series Symbol
A1	185	179	175	○
A2	630	631	604	□
A3	1110	1163	1060	◇
A4	1250	1006	998	△

The remaining five test series were performed with propellants B, C, D, E, and F:

Test Series	UTC Design Pressure	Theoretical Avg. Press.	Avg. Press. at 1.0 G	Series Symbol
B	780	863	762	⌂
C	680	695	642	◇
D	870	1052	865	⌂
E	450	542	447	▱
F	450	507	445	⬡

Since there was no burn rate augmentation measured with the non-metallized propellant (G) at the acceleration levels achieved during these test series, the results obtained with this propellant have not been included herein.

From the above, it is noted that there are some discrepancies between the UTC test pressure designation and the theoretical average pressures calculated from the UTC - supplied burn rate data. These discrepancies can most likely be attributed to erroneously high values of base burn rate.

Although the UTC grain is designed for neutral burning, the test results achieved at average accelerations of approximately 1.0 G indicate normally regressive burning. As illustrated in Figure 4-7, normalized pressure histories indicate a burning regressivity of as much as .78, with the largest deviations occuring during the first half of the burning interval. The cause(s) of these deviations from anticipated performance have not as yet been determined. However, recent motor extinction tests conducted at UTC have indicated that motor ignition is quite uniform over the propellant surface, thereby eliminating one likely source of the apparently non-uniform grain regression.

The influence of the spin environment on the nozzle mass flow coefficient (C_D) is illustrated in Figure 4-8. As indicated, values

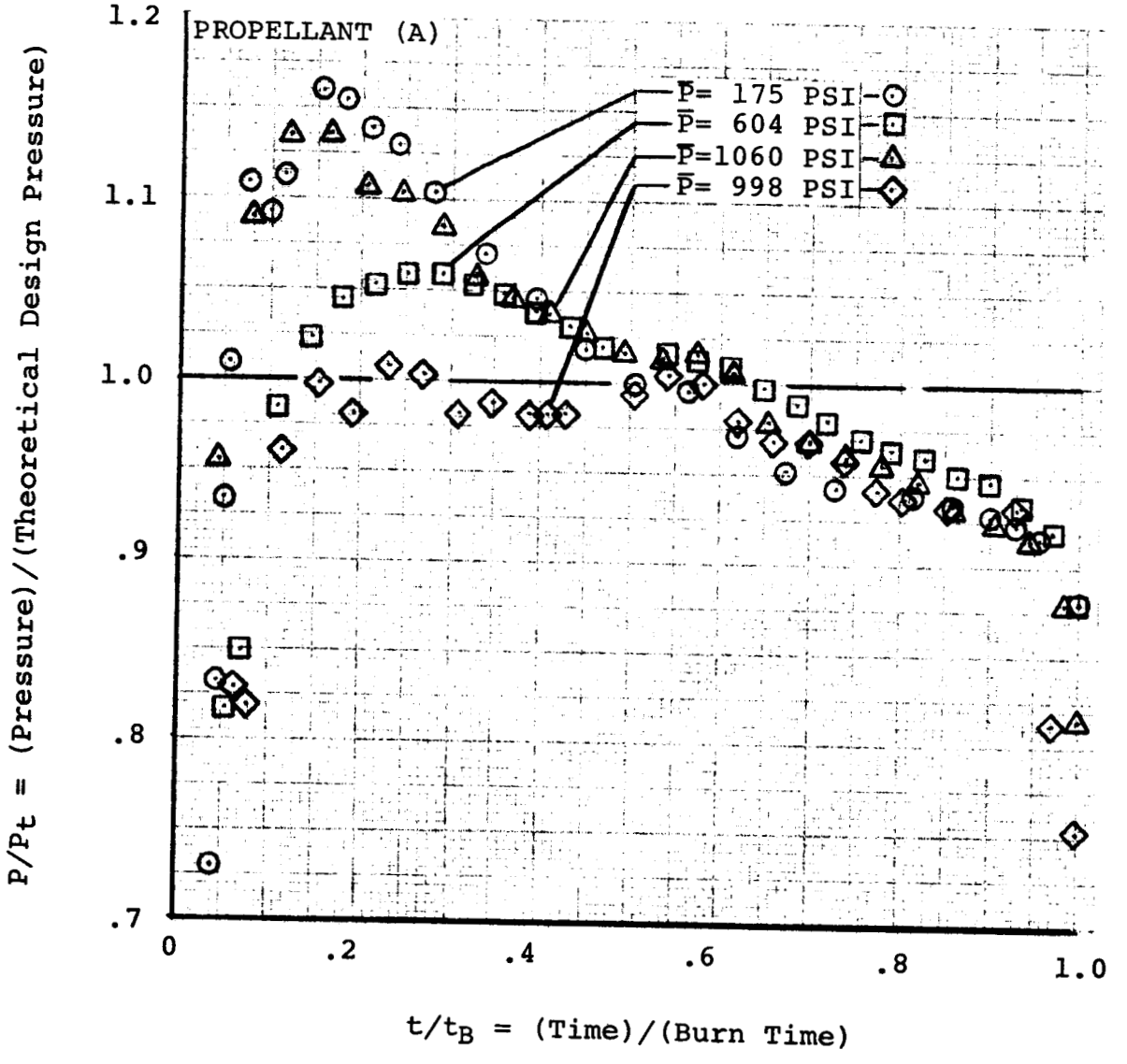

FIGURE 4-7: Propellant (A) Pressure Histories at 1.0 G

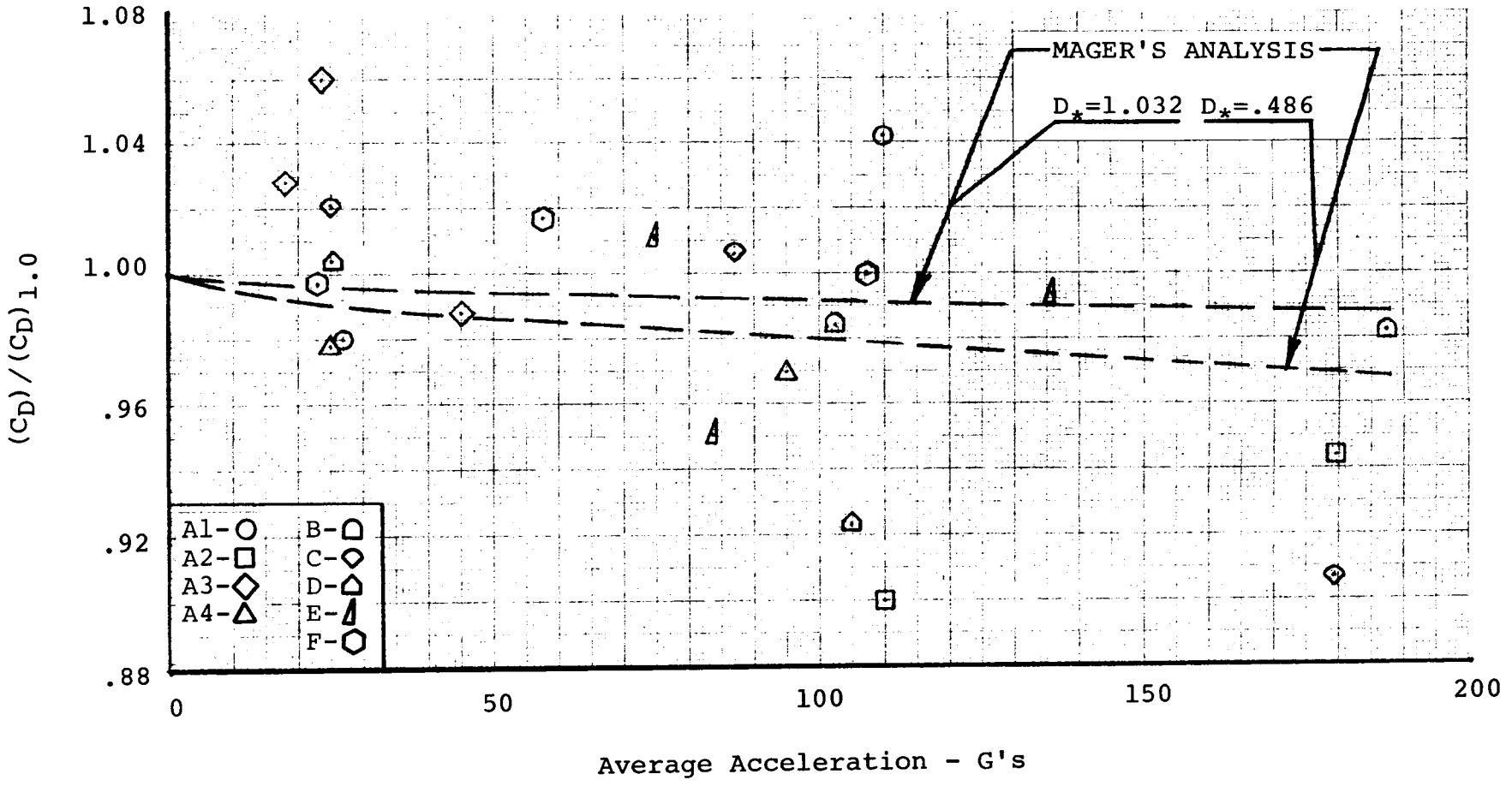

FIGURE 4-8: Variations in Nozzle Mass Flow Coefficient (C_D)

of C_D normalized with those obtained at 1.0 G do not generally vary monotonically with acceleration level. However, there does appear to be a trend toward lower values of C_D with increasing acceleration level. Assuming that the reduction in nozzle efflux capability in a spin environment can be attributed to an effective reduction in C_D, Figure 4-8 also gives the change in C_D predicted by Mager's analysis for irrotational flow (11).

As indicated in Figure 4-9, operating pressures averaged over burn time are found to increase with acceleration level in all instances, with those achieved by the CTPB binder propellant (F) exhibiting the greatest increases at the lower accelerations. With the exception of propellant (C) with the dichromated aluminum, all other propellant modifications are found to reduce the overpressures below those obtained with propellant (A).

The majority of the test results discussed below are presented graphically in the form of an instantaneous burn rate augmentation factor (r_r/r_t) given as a function of the percent of total mass efflux (m_o/m). As discussed in Appendix C, the instantaneous burn rate augmentation is given by:

$$[15] \qquad r_r/r_t = (\dot{m}_o/\rho S_r)/r_x(P/P_x)^n = (AF)_i$$

where r_r = the burn rate required to yield the "measured" mass flow rate ($\dot{m}_o = C_D P A_*$) with a propellant surface area of S_r (= 86.6 IN^2) and a density (ρ) determined by the initial propellant mass (m_p) and web thickness (W) according to: $\rho = m_p/WS_r$.

and r_t = the theoretical burn rate at the measured operating pressure (P).

Thus $(AF)_i$ provides a measure of the actual burning rate required to yield the measured value of combustion pressure compared to that which would be realized at such a pressure with no acceleration-induced burn rate augmentation.

As indicated in Figure 4-10, the burn rate augmentation experienced in series A1 (nozzle throat diameter = 1.032 IN) appears to increase with the percent of web burned, with some change in combustion characteristics noted in all three firings at 60-70% of the burning interval.

Essentially the same effects are noted in Figure 4-11 for Series A2 (nozzle throat diameter = 0.639 IN), except that the maximum augmentation experienced at 110 G's is approximately 15% greater than that realized at a comparable acceleration level but lower operating pressure in A1.

The reduction in $(AF)_i$ for series A-2 at 180 G's for $m_o/m > 45$-50%

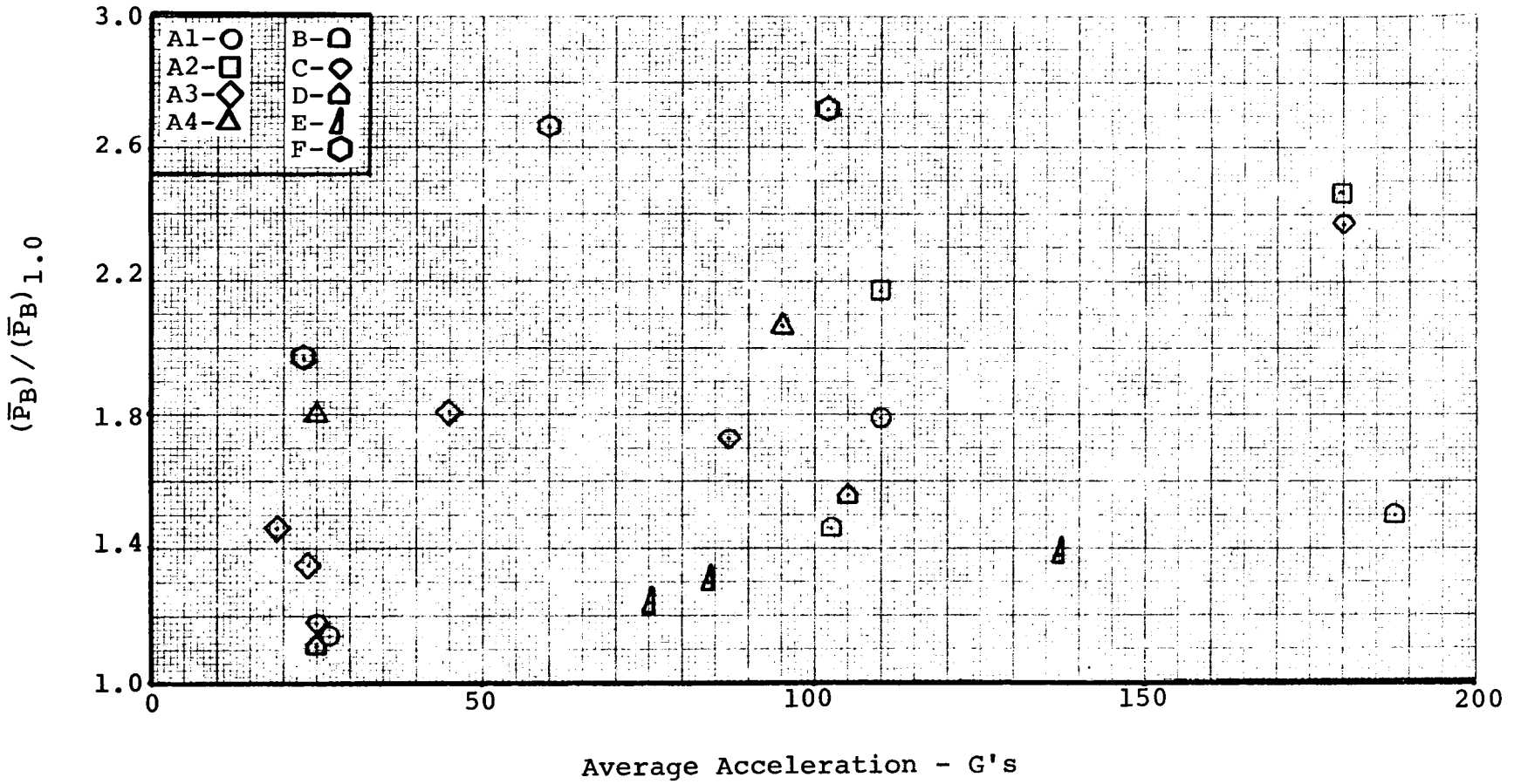

FIGURE 4-9: Variations in Average Combustion Pressure Over Burn Time

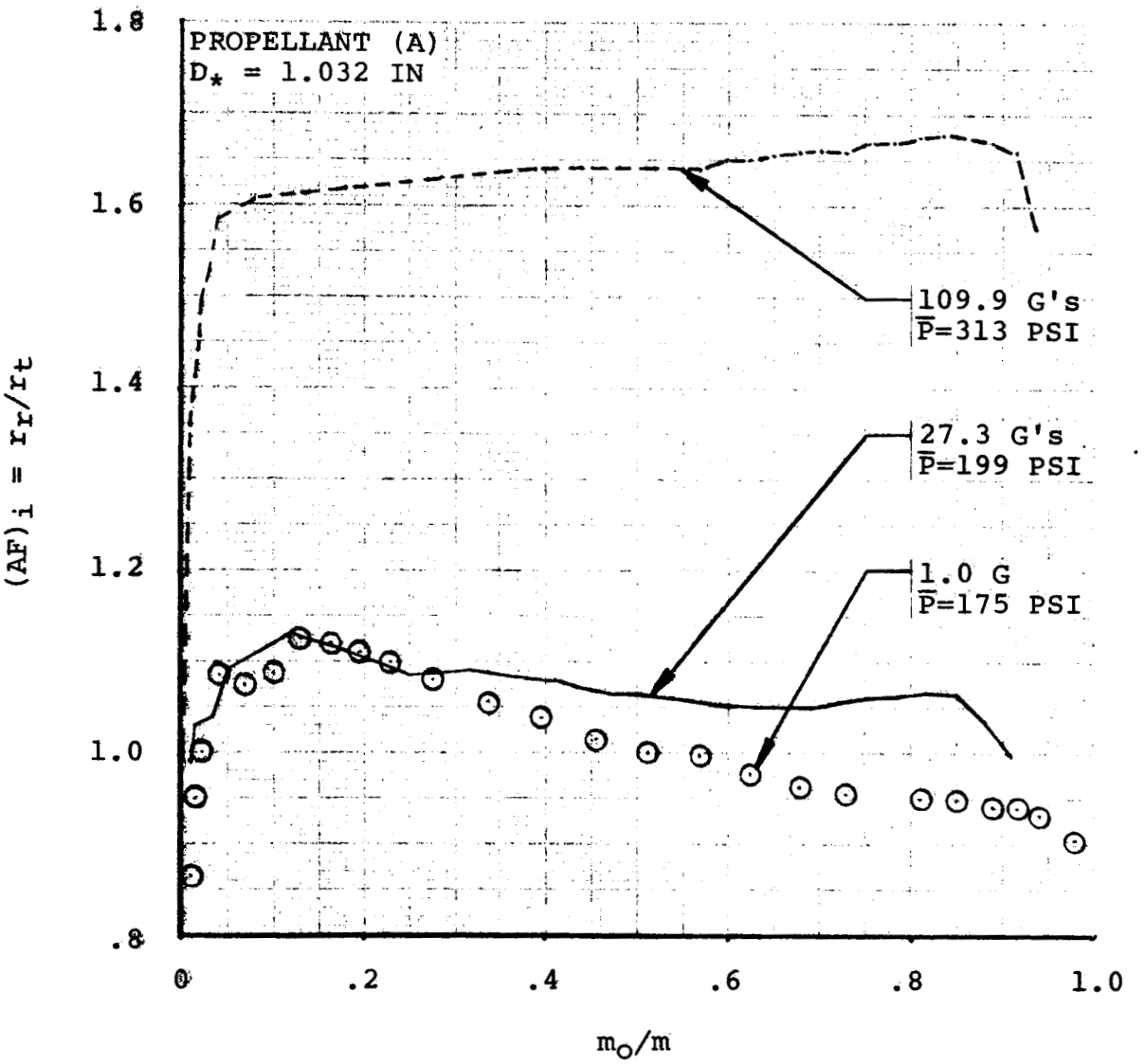

FIGURE 4-10: Burn Rate Augmentation for Series A1

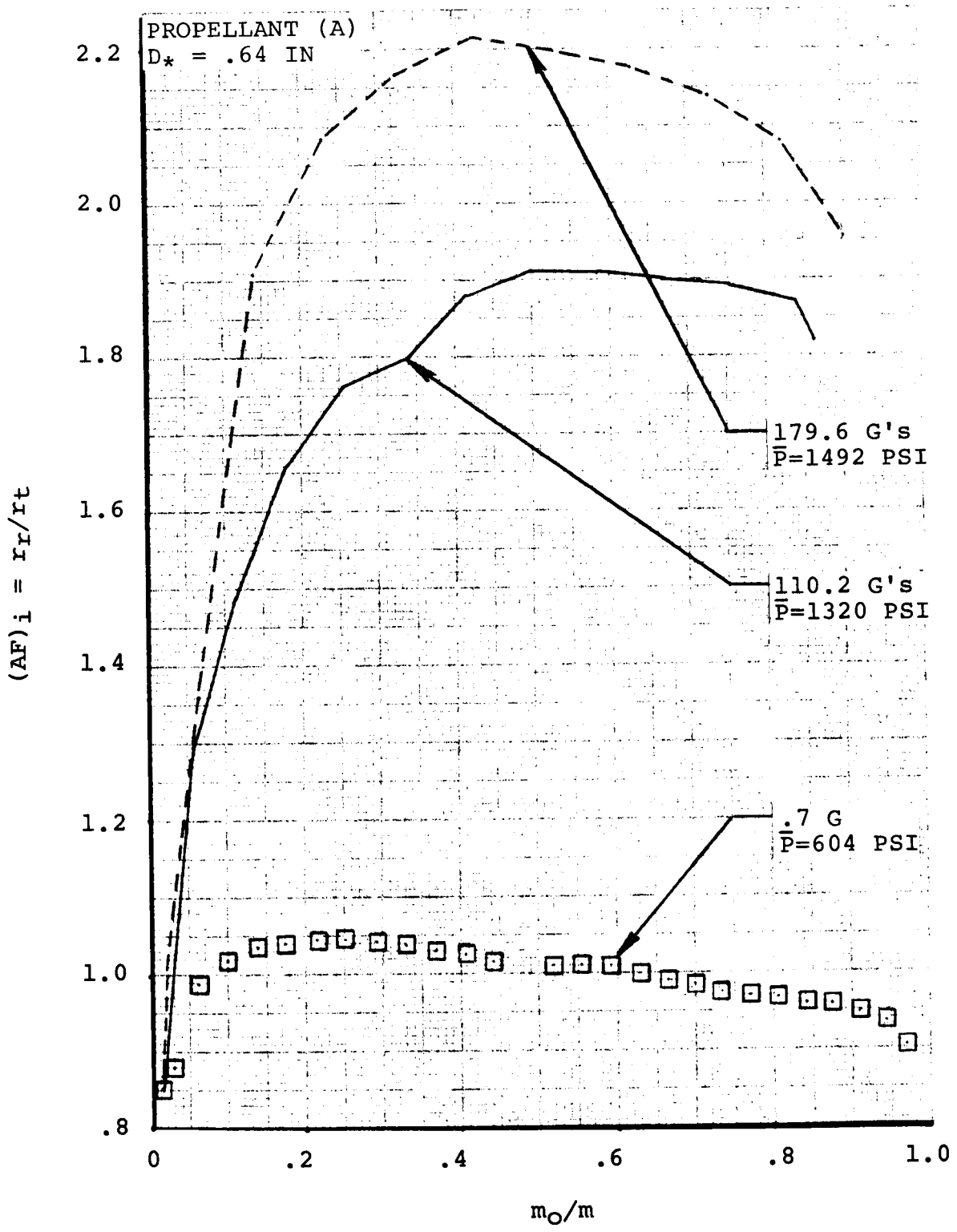

FIGURE 4-11: Burn Rate Augmentation for Series A2

is also evidenced in Figure 4-12 for series A3 (nozzle throat diameter = 0.486 IN) at a much lower acceleration level (45 G's) but higher operating pressure. Again, this change in burn rate augmentation is found to occur after about half of the web has been consumed.

Essentially similar transient behavior is also exhibited in Figure 4-13 for series A4 (nozzle throat diameter = 0.50 IN).

The effects of operating pressure on burn rate augmentation at essentially equivalent acceleration levels are illustrated in Figures 4-14 and 4-15. At 25 G's (Figure 4-14) increasing the operating pressure from 200 to 1500 PSI produces a 50% increase in maximum augmentation, while an increase to 1800 PSI yields no further augmentation, but apparently causes the point of maximum augmentation to occur at a smaller percentage of web burned. At 100 G's (Figure 4-15) this same transposition of the point of maximum augmentation is also evidenced with increasing pressure.

As indicated in Figures 4-16 through 4-20, results essentially equivalent to the above were also obtained with the various modifications of propellant (A). However, all modifications except the change from the PBAN to the CTPB binder generally resulted in lower burn rate augmentations.

The effects of the various propellant modifications at 100 G's are illustrated in Figure 4-21. As indicated, the reduction in AP particle size (D) yields generally lower augmentations than those achieveable by reducing the size of the aluminum particles (B). Conversely, the change from PBAN to CTPB binder systems yields a propellant which is much more sensitive to the spin environment.

As indicated in Figure 4-22, the use of dichromated aluminum (which theoretically reduces the tendency to form aluminum agglomerates at the propellant surface) produces a 16% reduction in maximum augmentation at an acceleration of 180 G's and essentially equivalent operating pressures.

Average values of burn rate augmentation $(\overline{AF})_i$ calculated from method [B] are compared to the burn rate augmentation factors (AF) obtained from method [A] in Table 4-1. As indicated in Section III and Appendix C, values of (AF) are determined by requiring that the measured propellant web thickness be totally consumed over the burning interval. That is,

$$(AF)\int_0^{t_B} r_X (P/P_X)\,dt = W$$

Values of $(\overline{AF})_i$ are obtained from:

$$(\overline{AF})_i = \int_0^{t_B} r_r\,dt \Big/ \int_0^{t_B} r_t\,dt$$

From the method used to determine r_r, it can be shown that

$$(\overline{AF})_i/(AF) = (m_o/m_p)_B$$

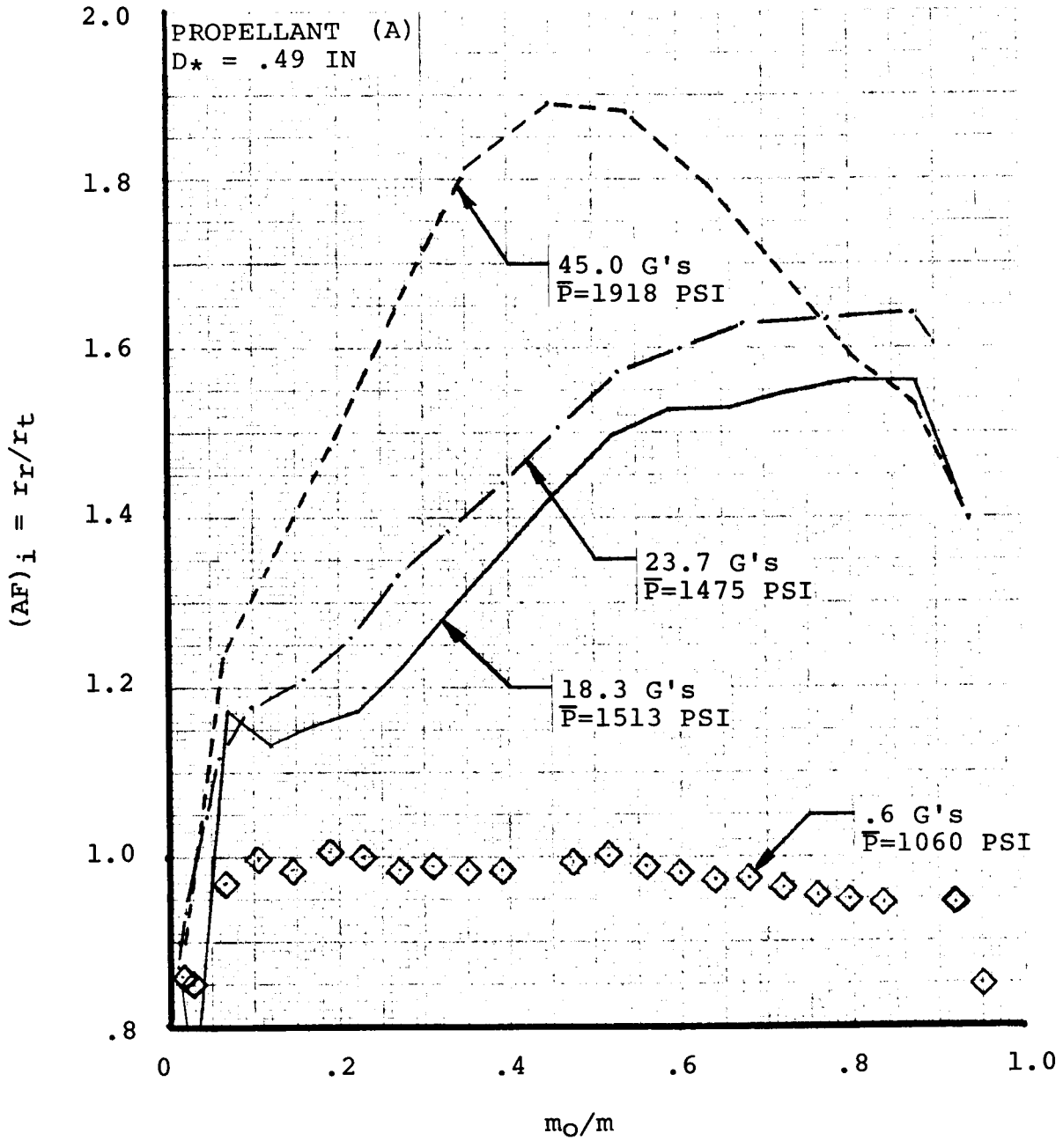

FIGURE 4-12: Burn Rate Augmentation for Series A3

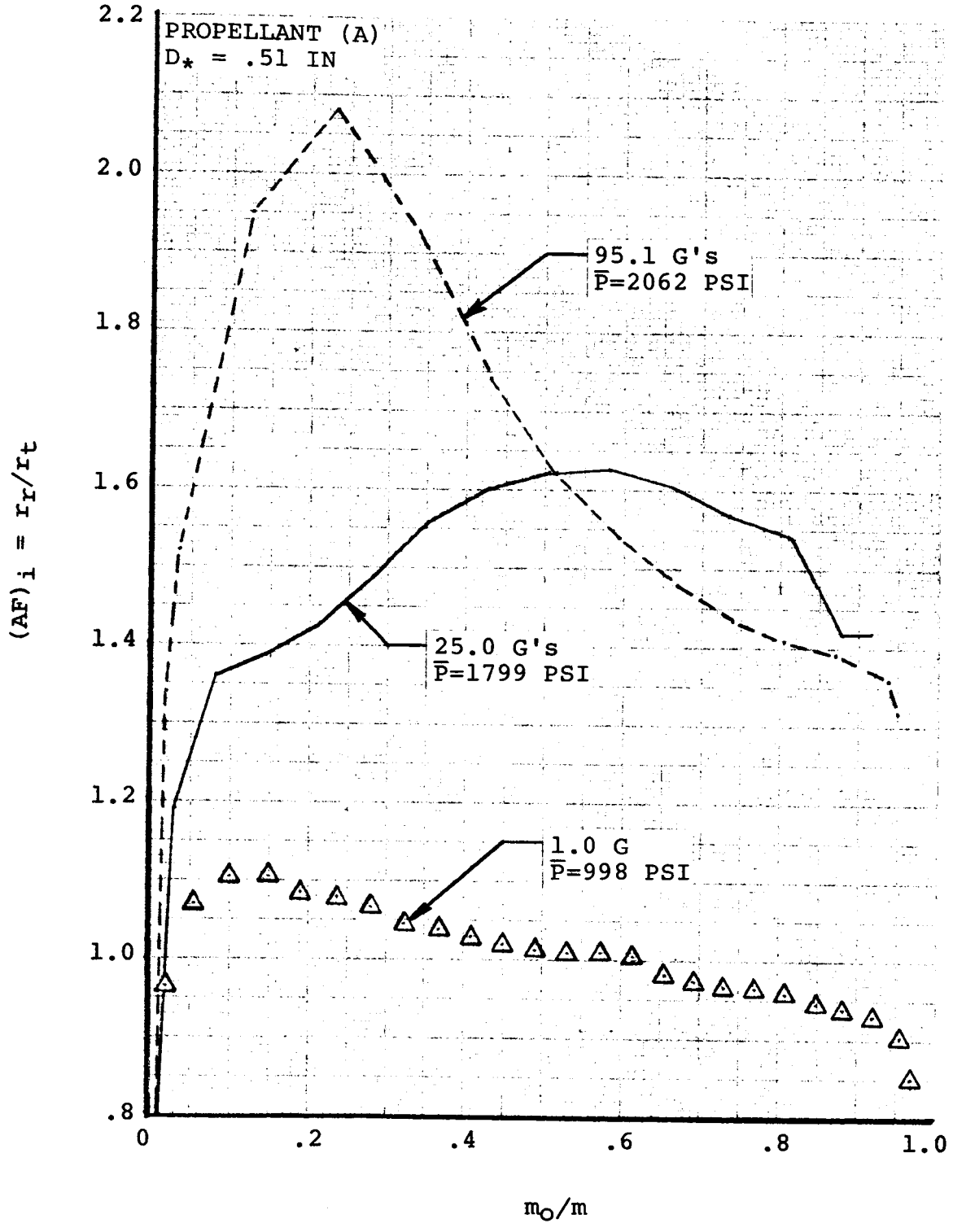

FIGURE 4-13: Burn Rate Augmentation for Series A4

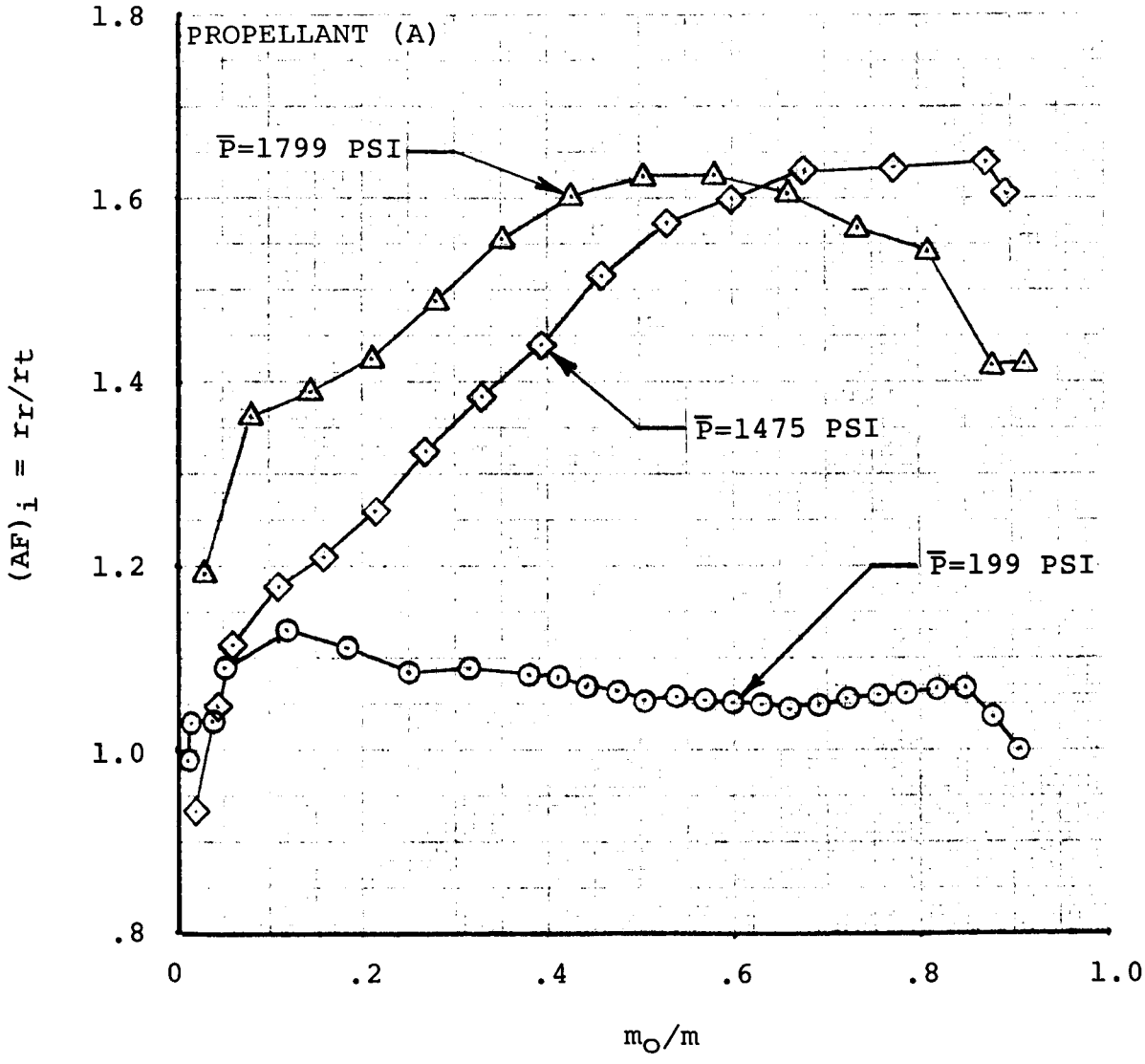

FIGURE 4-14: Pressure Effects on Burn Rate Augmentation -Propellant (A) at 25 G's Acceleration

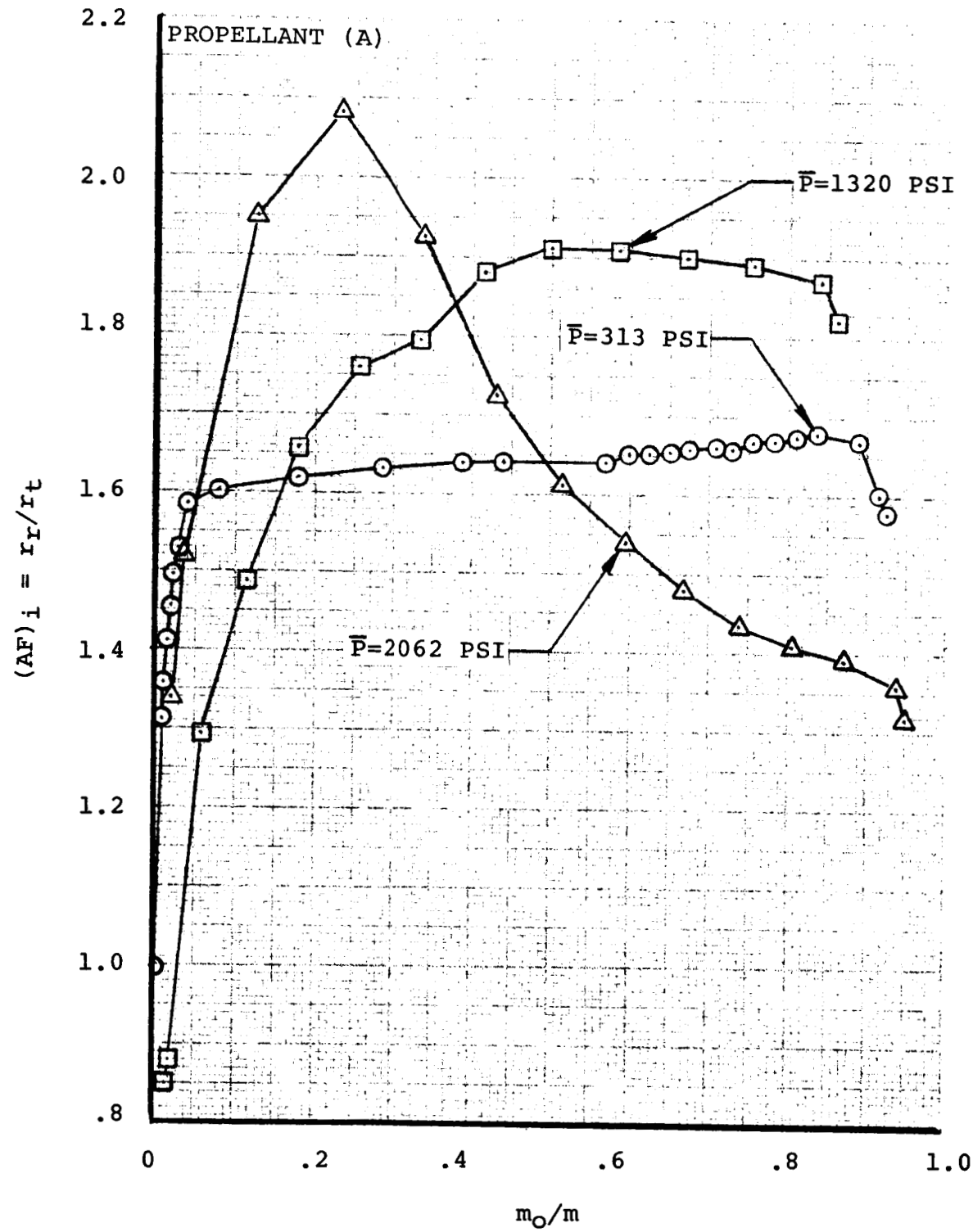

FIGURE 4-15: Pressure Effects on Burn Rate Augmentation -Propellant (A) at 100 G's Acceleration

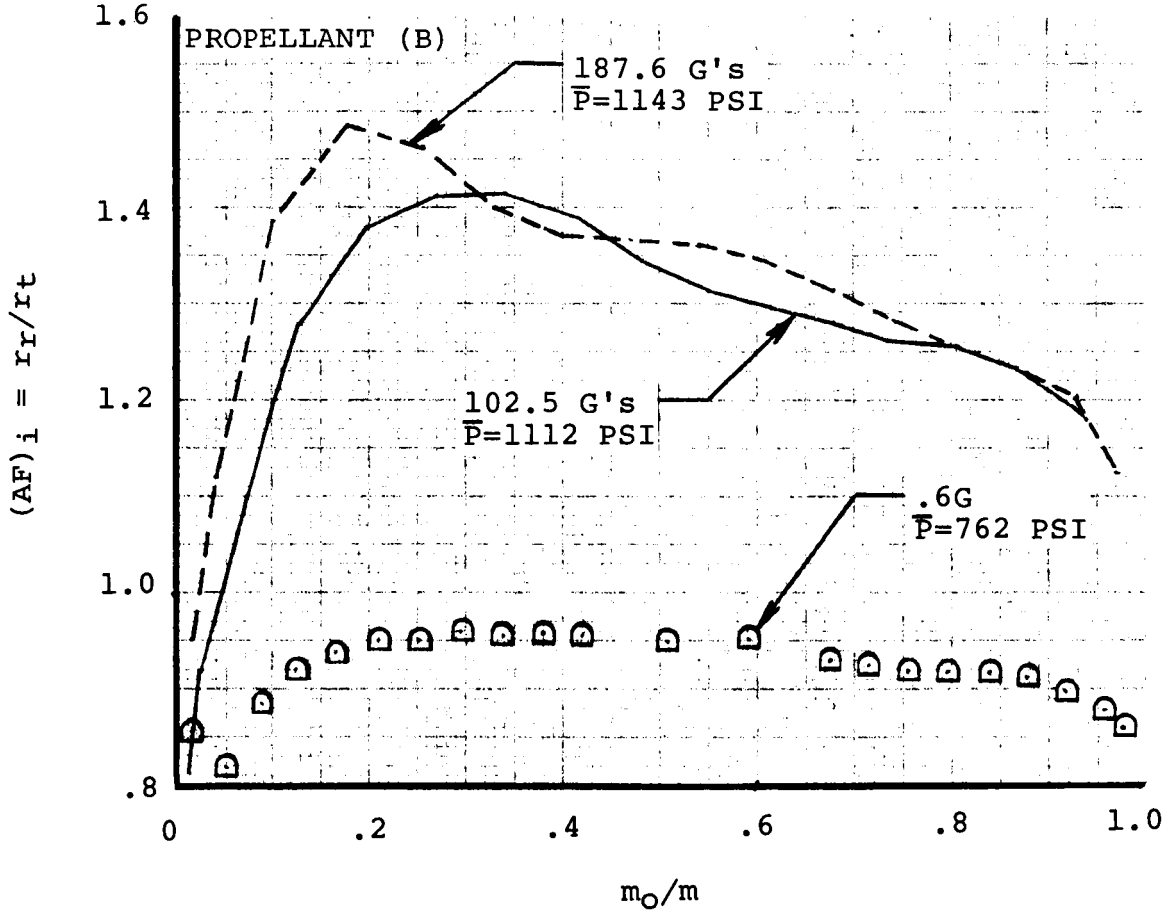

FIGURE 4-16: Burn Rate Augmentation for Propellant (B)

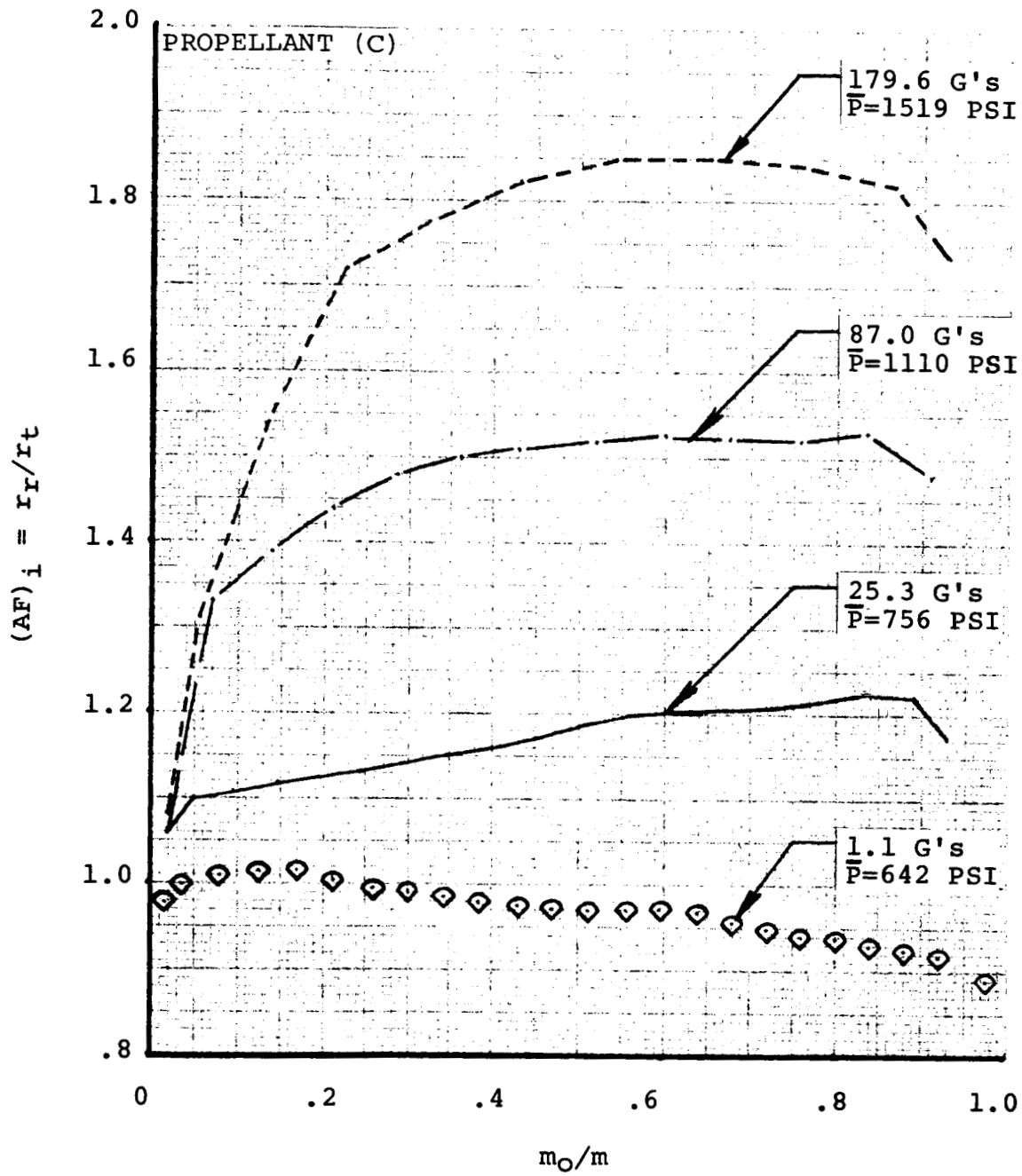

FIGURE 4-17: Burn Rate Augmentation for Propellant (C)

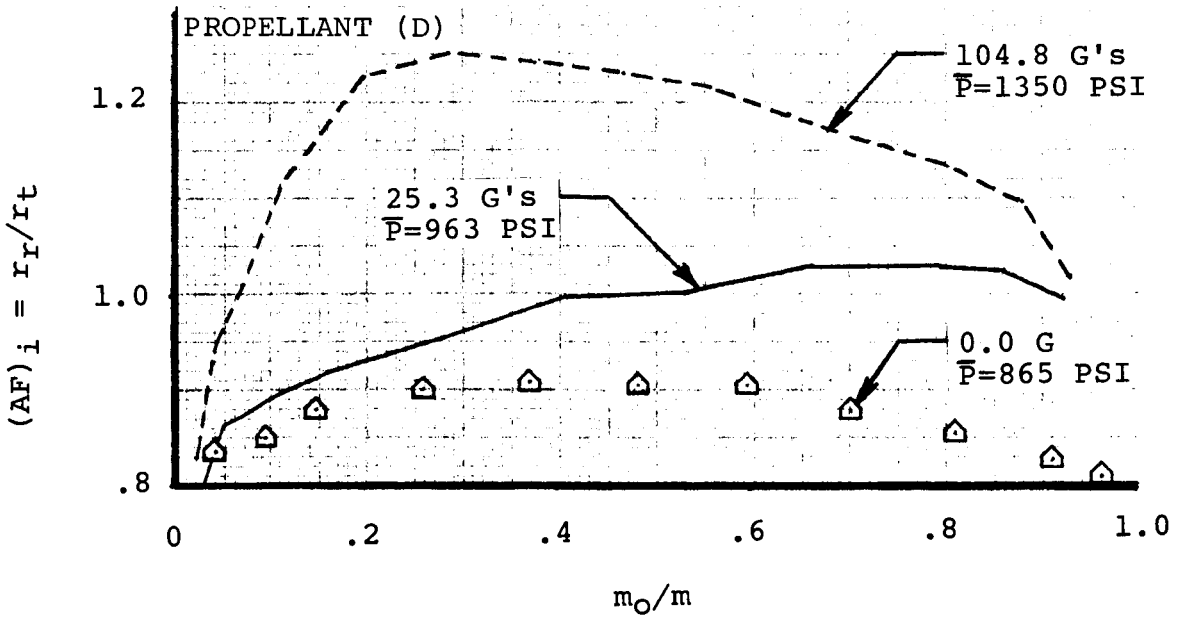

FIGURE 4-18: Burn Rate Augmentation for Propellant (D)

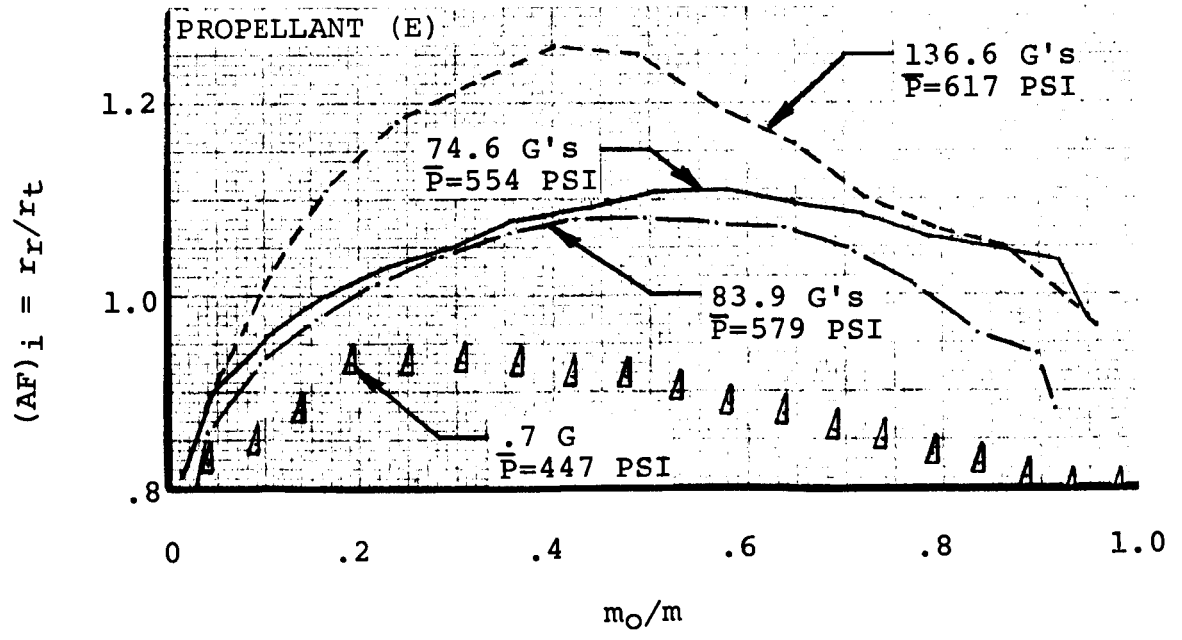

FIGURE 4-19: Burn Rate Augmentation for Propellant (E)

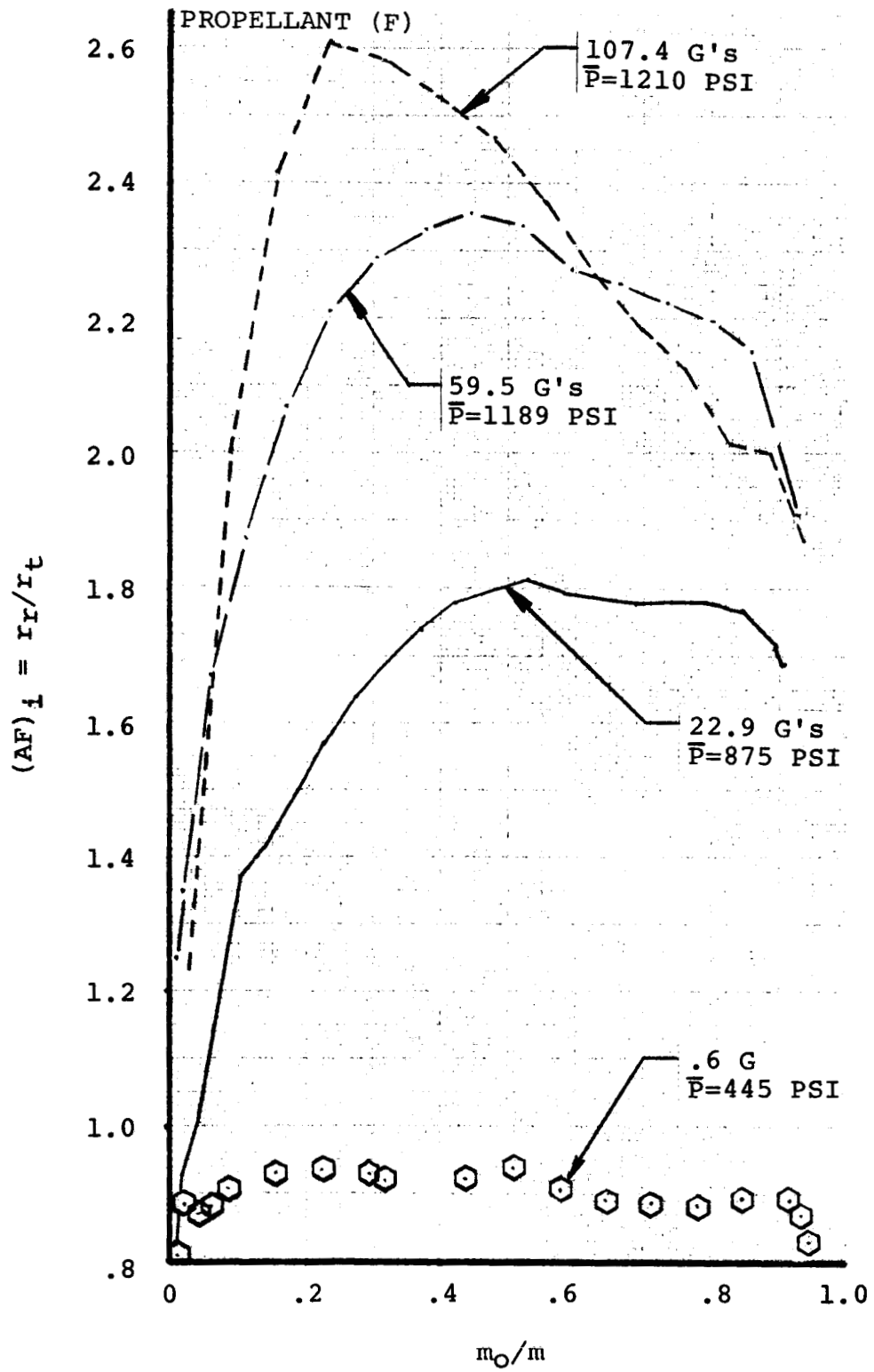

FIGURE 4-20: Burn Rate Augmentation for Propellant (F)

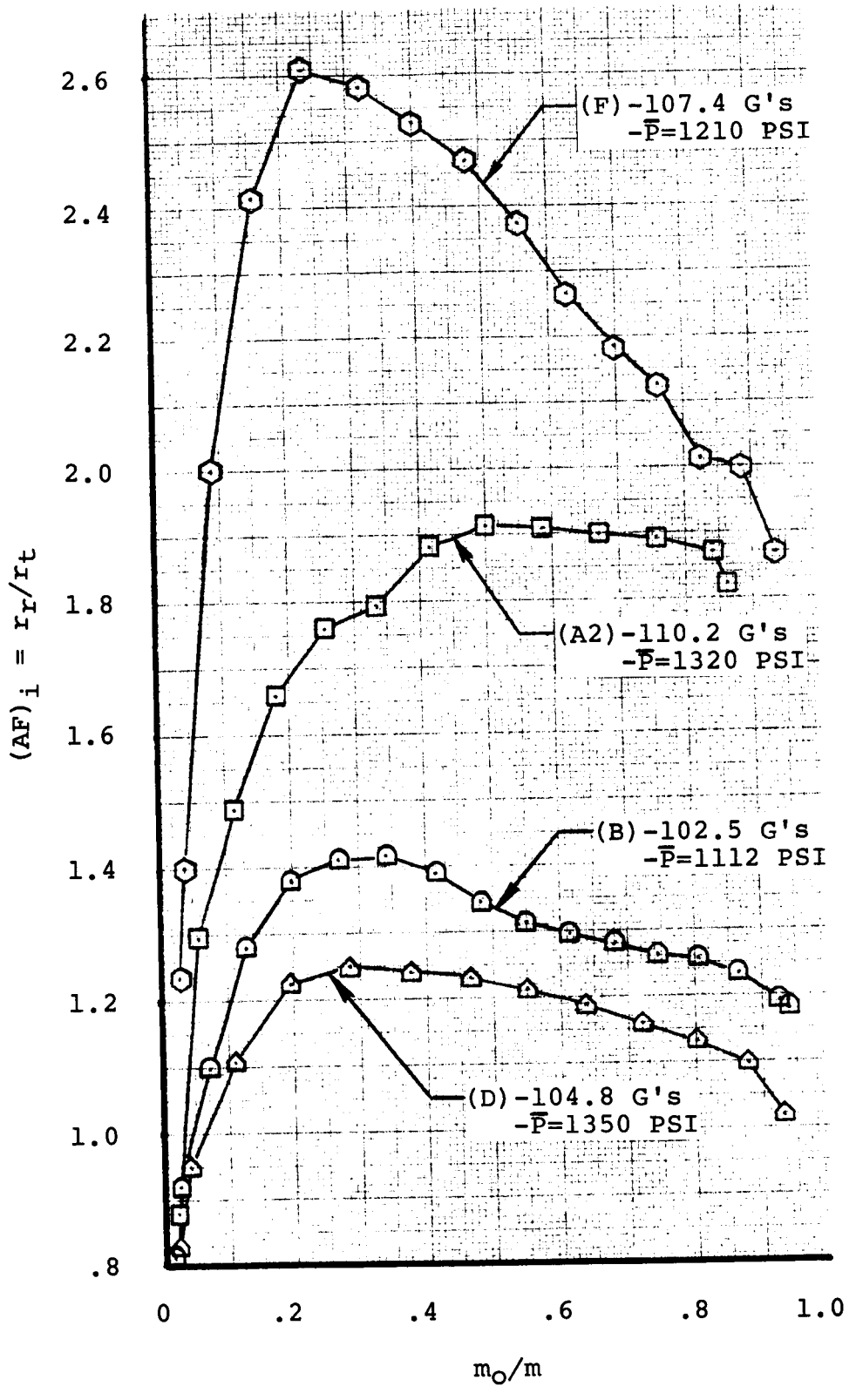

FIGURE 4-21: Effects of Propellant Modifications at 100 G's

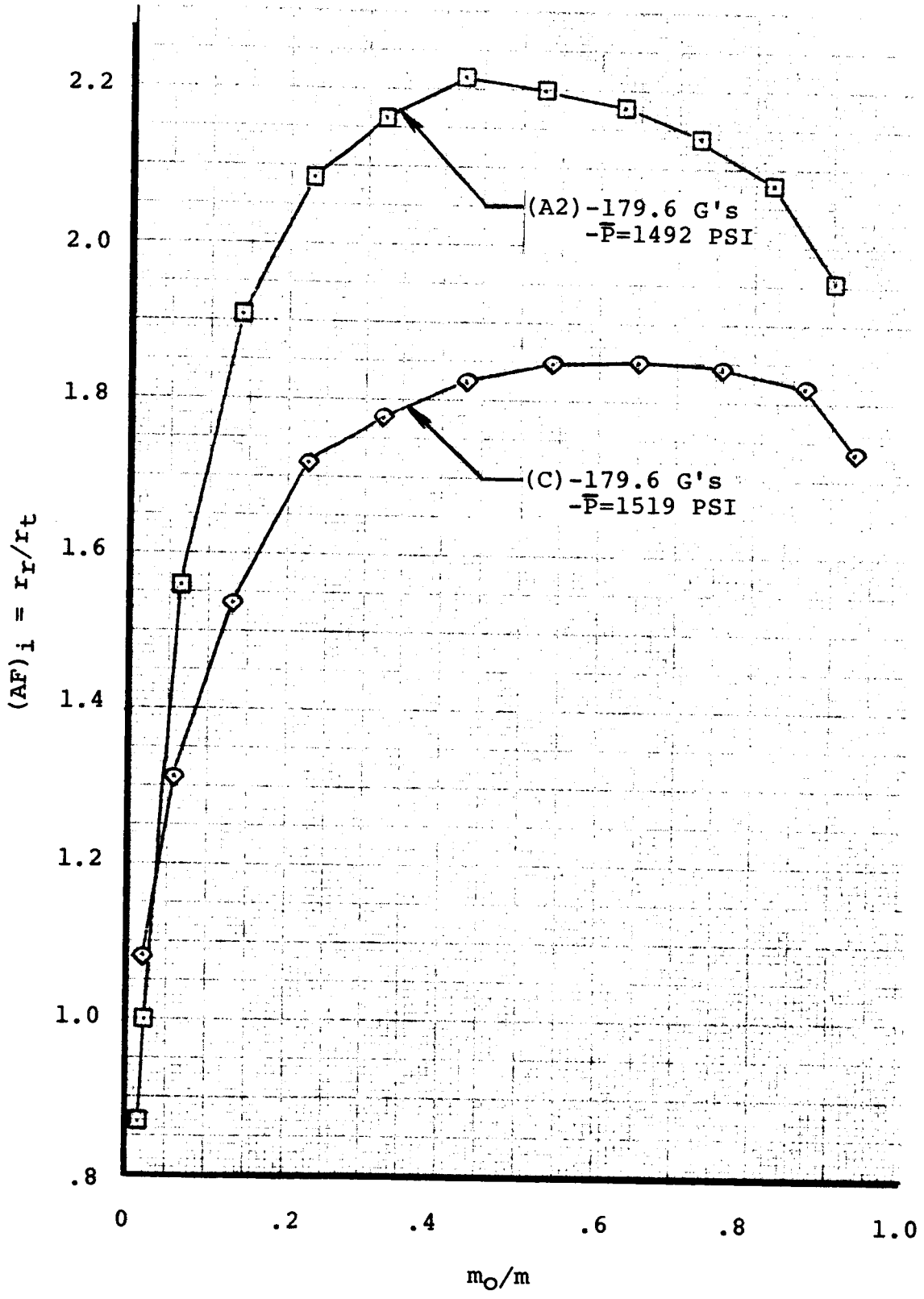

FIGURE 4-22: Effects of Propellant Modifications at 180 G's

TABLE 4-1: Burn Rate Augmentation Factors

Test Series	Average Acceleration (G's)	Average Pressure (PSIA)	$(\overline{AF})_i$	(AF)
A1	1.0	175	.948	.990
	27.3	199	1.064	1.231
	109.9	313	1.625	1.805
A2	.7	604	.971	1.017
	110.2	1320	1.656	1.972
	179.6	1492	1.912	2.174
A3	.6	1060	.938	.978
	18.3	1513	1.302	1.445
	23.7	1475	1.346	1.548
	45.0	1918	1.527	1.711
A4	1.0	998	.994	1.043
	25.0	1799	1.457	1.660
	95.1	2062	1.590	1.802
B	.6	762	.968	.939
	102.5	1112	1.237	1.380
	187.6	1143	1.282	1.402
C	1.1	642	.952	1.007
	25.2	756	1.136	1.248
	87.0	1110	1.421	1.600
	179.6	1519	1.633	1.803
D	0.0	865	.863	.899
	25.2	963	.948	1.048
	104.8	1350	1.124	1.263
E	.7	447	.864	.885
	74.6	554	1.029	1.116
	83.8	579	.993	1.117
	136.6	617	1.098	1.177
F	.6	445	.896	.974
	22.9	875	1.578	1.800
	59.5	1189	2.068	2.307
	107.4	1210	2.062	2.282

where $m_o = {}_c\int^{t_B} C_D P A * dt$
and m_p = the initial mass of propellant = $\rho W S_r$

In order to eliminate the discrepancies in the burn rate data provided at 1.0 G, values of $(\overline{AF})_i$ normalized with those obtained at 1.0 G are given in Figure 4-23. As indicated, all propellant modifications except the change from PBAN to CTPB binder systems have reduced the burn rate augmentation in the spin environment. At 25 G's, reducing the AP particle size (△) is more effective than using dichromated aluminum (◇). However, the significance of motor operating pressure is evidenced by the fact that the results obtained with propellant (A) operating at 200 PSI (○) are essentially equivalent to those achieved at 960 PSI by reducing the AP particle size (△). At 100 G's, reducing the size of the Al particles (□) is found to yield a reduction in burn rate augmentation equal to that provided by reducing the AP particle size (△). However, a further reduction is achieved with the addition of 1% Fe_2O_3 to increase the base burn rate of the propellant (◭).

In summary, the UTC test results discussed above have indicated that burn rate augmentation in a spin environment is dependent upon:

(1) Acceleration Level - All tests have yielded increasing motor operating pressures with increasing centrifugal acceleration levels. Although these operating pressures appear to be approaching asymoptotic values in some instances, this observation is not borne out with all formulations over the 0 to 200 G acceleration levels examined herein.
(2) Operating Pressure - At a constant acceleration level, the burn rate augmentation experienced with a given propellant formulation appears to increase with combustion pressure.
(3) Web Burned - Practically all pressure histories were progressive-regressive with a grain designed for neutral burning. For a given acceleration level and propellant formulation, the percent of web burned at the point of maximum pressure is inversely proportional to operating pressure. Similarly, the percent of web burned at maximum pressure is inversely proportional to acceleration level for each variation in the propellant formulation.
(4) Particle Size - Reducing the size of either the AP or Al particles caused significant reductions in burn rate augmentation at a given acceleration level. Which of the two modifications is more effective has not been established.
(5) Base Burn Rate - Burn rate augmentation is inversely proportional to base burn rate.
(6) Binder System - The change from the basic PBAN to CTPB binder system caused a dramatic increase in acceleration sensitivity, particularly at the lower acceleration levels.

Thus the results of this study (as well as similar results recently published by the Naval Postgraduate School (15) and others soon to be published by Langley Research Center) have rather conclusively established that practically every propellant formulation variable and motor operating condition will have an influence on motor performance in a spin environment.

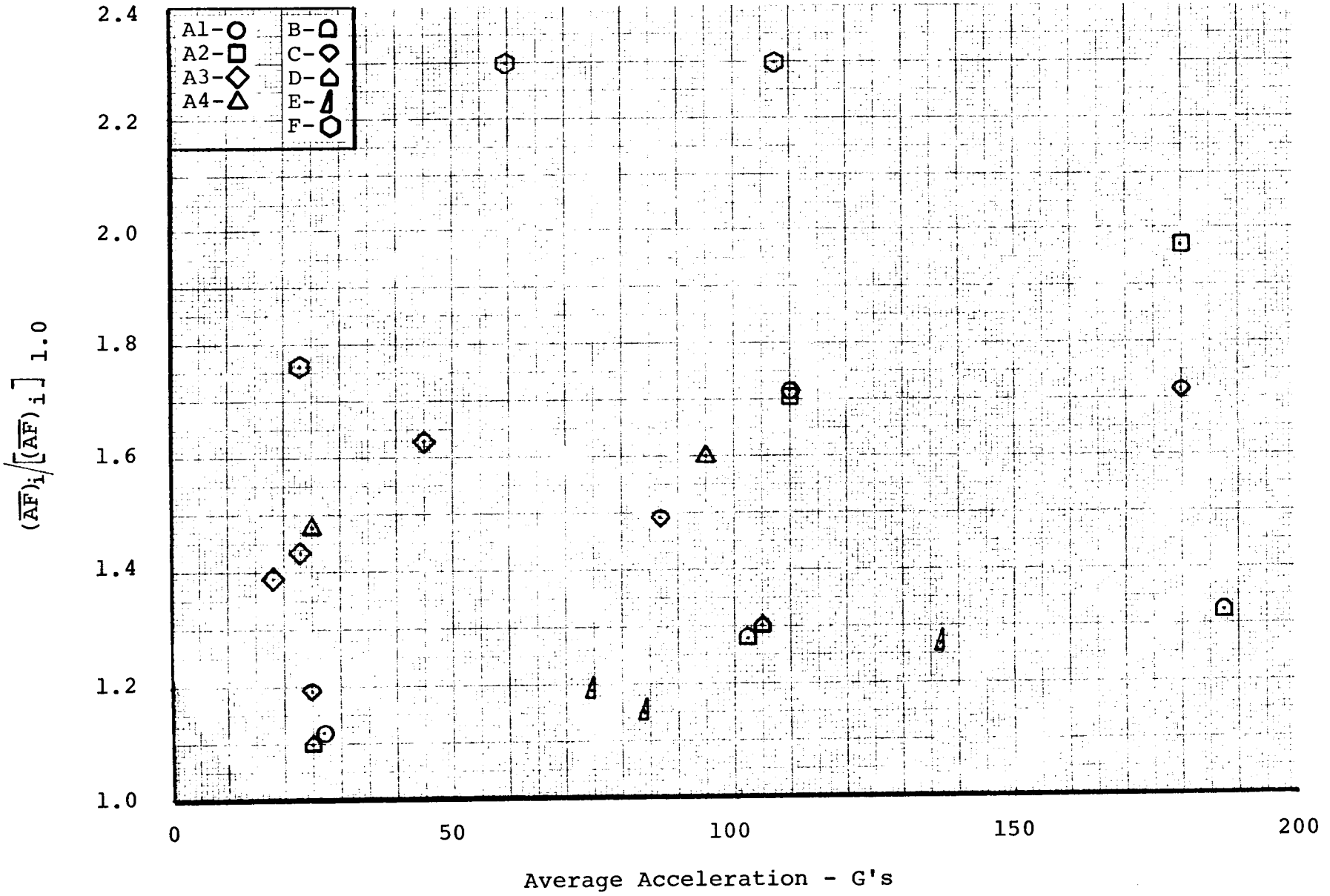

FIGURE 4-23: Normalized Average Burn Rate Augmentations

SECTION V

CONCLUSIONS AND RECOMMENDATIONS

As illustrated in Volume II of this report, numerous performance anomalies have been experienced with the majority of the developmental solid propellant rocket motors operating in spin environments. Therefore, beginning about 1965, non-developmental acceleration research studies were initiated at the NASA Langley Research Center (LRC), the U. S. Naval Postgraduate School (NPS), and United Technology Center (UTC) in an effort to develop an understanding of the phenomena involved and to identify the significant variables causing the observed deviations from static performance. In general, these studies have shown that all propellants are affected by acceleration environments. In some instances, there is a threshold acceleration level below which propellant performance is not affected. In others, there is apparently an upper limit to acceleration sensitivity, beyond which propellant performance remains essentially constant. Moreover, motor performance in a spin environment is further complicated by changes in nozzle flow characteristics, which compound the already complex combustion phenomena.

Combustion Phenomena

All three principal investigators of acceleration effects on propellant combustion characteristics agree that accelerations directed normally into the surface of a composite propellant will cause an increase in the apparent burning rate of the propellant. However, it has not as yet been firmly established whether this increase in regression rate is due primarily to localized "pocking" of the propellant surface which causes an increase in burning surface area, or to an overall increase in burning rate. Motor extinction tests conducted at both LRC and UTC have indicated severe surface "pocking" in some instances, but essentially smooth surfaces in others. Based upon this evidence and the results of his studies at the NPS (15), Sturm has postulated the existence of two distinct combustion modes for aluminized propellants: (a) a fast-burning mode in which distinct agglomerates of aluminum determine the burn rate and increase in surface area; and (b) a slower mode in which the surface is essentially flooded with aluminum oxide.

As exemplified by the UTC test data included in Section IV, results obtained with aluminized propellants indicated that the burn rate augmentation induced by acceleration can be reduced by: (a) increasing the base burn rate of the formulation by the addition of burn rate catalysts; and/or (b) reducing the size of either the Al or AP particles in the propellant composition. However, in developing his model describing acceleration effects on non-metallized propellants (15), Sturm cautions that the beneficial effects of reducing the AP particle size cannot necessarily be extrapolated to non-aluminized propellants.

Although these and other qualitative conclusions have been confirmed by all three investigators, their studies have not yet yielded any quantitative methods of predicting propellant sensitivity to acceleration other than Sturm's model for non-aluminized propellants and by a theory developed by Crowe and Willoughby of UTC for aluminized formulations. Unfortunately, both of these models require normally unavailable knowledge of essentially the microscopic combustion characteristics of the propellant ingredients to allow prediction of the macroscopic acceleration sensitivity.

Without question, progress toward understanding combustion phenomena in an acceleration environment has been hindered by two primary factors: (a) the inability to control the burning environment; and (b) the inability to view the burning surface during the combustion process.

Each of the three principal investigators of acceleration phenomena has employed a different experimental technique to determine burn rate augmentation. As indicated in Section IV, UTC has used spin tests of a tapered cylindrical grain. LRC has used centrifuge tests of a 0.5 IN thick slab motor with a 24 IN^2 burning surface area. The NPS has also used a centrifuge to provide the acceleration force, but employs 0.24 IN square propellant strands of varying length as the test items.

As is obvious from the UTC test results discussed previously, spin testing has three distinct disadvantages:

(1) Combustion pressure cannot be controlled during firing to allow segregation of effects due to pressure from those due primarily to the acceleration field.

(2) Gas vortexing effects and changes in nozzle efflux due to the spin environment cannot be divorced from the combustion phenomena, primarily because there is currently no verified analytical method available for predicting spin effects on rocket motor gas dynamics.

(3) While operating at a constant spin rate, the centrifugal acceleration at the propellant surface increases (37% in the UTC tests) as the internal grain diameter increases during burning. If the spin rate is decreased during the test to maintain a constant centrifugal acceleration, unwanted radial accelerations are developed. Moreover, such a programmed decrease in spin rate requires pre-test knowledge of motor burn time, which may vary by factors of 2.0 or more depending on acceleration level.

In addition, spin testing also suffers the disadvantage of not being able to determine propellant sensitivity to the angle between the propellant surface and the acceleration vector, which Northam of LRC has demonstrated to be a very significant factor in determining burn rate augmentation (16).

The LRC centrifuge slab motor tests have effectively eliminated the second and third disadvantages of spin testing, and do provide for varying the propellant surface orientation with respect to the acceleration vector. However, this test technique also suffers the serious disadvantage of not being able to control combustion pressure during burning.

The NPS centrifuge strand tests have effectively eliminated all the disadvantages of spin testing by providing a plenum to allow combustion at essentially constant pressure. However, the small dimensions of the burning surface (0.25 IN x 0.25 IN) and encapsulation of the burning residue by the inhibitor "walls" of the strands could have considerable influence on the test results and their interpretation, particularly since the dimensions of the "pocked" areas observed in some of the LRC slab extinguishment tests are of the same order of magnitude as the total NPS burning surface.

If the effects of acceleration environments on the solid propellant combustion process are ever to be determined quantitatively on a macroscopic scale, the experimental test procedures employed in this attempt will have to incorporate:

(1) Control of the combustion pressure during burning to increases of less than 10%.

(2) Control of the acceleration levels between tests to differences of less than 5%.

(3) Control of the acceleration level during burning to changes of less than 5%.

(4) Temperature control of the test specimen to within $\pm 10^{\circ}F$.

(5) Provision for orienting the propellant surface at angles from $\pm 90^{\circ}$ to the acceleration vector.

(6) Provision for (optically or electronically) determining the burning surface regression as a function of time.

(7) Provision for photographically recording the combustion process.

(8) Provision for acceleration levels up to a minimum of 500 G's.

(9) Provision for varying combustion pressure over a range of at least 200 - 2000 PSIA.

Incorporating all the above characteristics in a single test device would appear to necessitate the use of a centrifuge, similar to that already available at the NPS but with a greatly expanded capability for pressure control with much larger test specimens.

As a compromise between plenum requirements and the surface "pocking" characteristics already noted in the LRC and UTC tests, it would appear that test samples at least 2.0 IN in diameter and up to 3.0 IN in length should be able to be accomodated.

Although the ability to view the burning surface during combustion will not likely yield any quantitative data, providing this capability should accelerate the development of new combustion models or the revision/verification of current theories. This is particularly true with respect to UTC's most recent model for aluminized propellants, which requires knowledge of the agglomeration mechanism and agglomerate size as input data.

To this end, UTC is currently using a centrifuge-mounted combustion bomb for photographic studies of strand burning under acceleration. The results of these studies are to be published in the final report of their current contract for the Navy (14).

The test requirements outlined above are primarily designed to develop a more comprehensive understanding of the solid propellant combustion process and the effects of acceleration on this process. Judging from the progress to date in attempting to define solid propellant combustion mechanisms without acceleration, it would seem that the development of useful models for combustion in acceleration fields will be a lengthy process. However, it is quite possible that closely controlled acceleration studies may well provide the key to an improved understanding of the complete combustion mechanism.

At present, the designer of a solid propellant rocket motor which is to operate in a spin environment is left little choice but to test the proposed propellant formulation in an environment closely simulating that anticipated. If the effects noted are too severe, the studies performed to date have shown that propellant sensitivity can be reduced by reducing the size of the Al or AP particles or by increasing the base burn rate of the propellant. If these relatively minor modifications are not sufficiently effective, a change to a different type of binder system is indicated. However, there is currently little data available which describes the effects of acceleration on different binder systems.

As is obvious from the UTC test results presented in Section IV, the change from a CTPB binder system to a PBAN system produces a much greater reduction in acceleration sensitivity than any of the modifications of the PBAN system. However, the reason(s) for this gross change are unknown.

Therefore, in order to provide the motor designer with an improved basis for preselecting a propellant most suitable for operation in a spin environment, it is recommended that an investigation of acceleration effects on different binder systems be initiated. In order that this investigation yield something more than the usual

qualitative observations, it is further recommended that this study include attempts to correlate acceleration sensitivity with: (1) erosion sensitivity; (2) propellant mechanical properties; and (3) burn rate sensitivity to strain. Moreover, whereas most test data obtained to date has been limited to temperatures approximating 70°F, this investigation should include the full spectrum of anticipated operating temperatures.

Gas Dynamics

The influence of a spin environment on combustion chamber and nozzle gas dynamics further complicates the acceleration effects on the combustion process. The apparent reduction in nozzle efflux capability with spinning internal- or end-burning motors causes an increase in combustion pressure. Moreover, in some instances, severe erosion of the motor head closure has been noted with internal-burning grains, while end-burning motors have experienced severe centerline coning of the propellant surface, as illustrated in the MICOM test results discussed in Section IV.

Studies to develop methods of analytically predicting the spin influence on gas dynamics have been conducted primarily by the Purdue University Jet Propulsion Center (JPC), and more recently by UTC. Sponsored by the MICOM Propulsion Lab since July 1964, the JPC effort has included both analytical and cold-gas experimental studies of spin effects on the gas dynamics associated with simulated end-burning and cylindrical-burning grain configurations. The more recent Navy-sponsored program at UTC has concentrated on flow visualization studies of a simulated end-burning grain. The results of these and other related efforts are reviewed in Volume II of this report.

Although the studies conducted to date have rather firmly established that nozzle efflux capability can be significantly reduced in a spin environment, progress toward developing a comprehensive understanding of spinning gas dynamics has not been impressive. This situation is primarily due to the extremely complex nature of the generally three-dimensional (and often unsteady) flow phenomena involved, and complicated by the fact that the experimental measurement techniques employed frequently disturb the flow patterns to such an extent that the resultant measurements are worthless.

Although the combustion studies discussed previously are essential to quantifying the effects of spin on motor performance, a satisfactory description of motor behavior in a spin environment will not be achieved until the effects on motor gas dynamics have been evaluated and understood. In turn, this evaluation can be accomplished only by a thorough investigation of the analytical equations of motion governing gas behavior, in conjunction with selected experiments to validate or modify the results of these analyses.

In general, the results of the analyses performed to date have indicated that viscous effects are significant in determining the behavior of spinning gases. Therefore, it is recommended that an investigation of the complete Navier-Stokes equations be initiated, and directed toward application to both the rotational flow emanating from end-burning grains and the essentially irrotational flow emanating from cylindrical-burning grains. The objectives of this investigation would be twofold: (1) to quantify the reduction in nozzle efflux capability; and (2) to determine the mechanism(s) by which highly erosive velocities are developed at the centerline of an end-burning grain. The method of analysis would involve generating numerical solutions to the equations of viscous-gas motion for specific grain/nozzle geometries and, with these, developing similarity parameters suitable for normalizing the results in non-dimensional form.

Verification and/or modification of the above analyses would be accomplished primarily by means of cold-gas tests, performed in non-spinning test fixtures in order to allow maximum ease of instrumentation. Spin velocities would be simulated by drilling the gas inlet ports at varying angles to the motor (fixture) axis.

In conjunction with the combustion experiments, this comprehensive analytical/experimental program to define the effects of spin on motor gas dynamics should allow the solid propellant motor designer to predict the total effects of a spin environment on motor performance with a minimum of testing and re-design.

SECTION VI

REFERENCES

(1) "Compilation of Spin Data Program, Technical Summary No. 1"; Emerson Electric Co. Report No. 2122-1; 31 January 1967; (U).

(2) "Compilation of Spin Data Program, Technical Progress Report No. 4"; 7 March 1967; (U).

(3) "Compilation of Spin Data Program, Technical Progress Report No. 5"; 6 April 1967; (U).

(4) "Compilation of Spin Data Program, Technical Progress Report No. 6"; 1 May 1967; (U).

(5) "Compilation of Spin Data Program, Technical Progress Report No. 7"; 1 June 1967; (U).

(6) "Compilation of Spin Data Program, Technical Progress Report No. 11"; 10 October 1967; (U).

(7) L. J. MANDA: "Compilation of Rocket Spin Data Final Report, Volume II - Literature Survey"; Emerson Electric Co. Report No. 3001-2; July 1968; (U).

(8) "Compilation of Spin Data Program, Technical Progress Report No. 14"; 9 January 1968; (U).

(9) W. D. GUTHRIE and D. R. ULLOTH: "A Study of Vortex Effects in Spinning Rocket Motors"; Report RK-TR-66-8; April 1966; AD-374624; (C).

(10) L. J. MANDA: "Spin Effects on Rocket Nozzle Performance"; AIAA Journal of Spacecraft and Rockets; Volume 3, No. 11; November 1966; pp. 1695-1696; (U).

(11) A. MAGER: "Approximate Solution of Isentropic Swirling Flow Through a Nozzle"; ARS Journal; Volume 31, No. 8; August 1961; pp. 1140-1148; (U).

(12) C. T. CROWE and P. G. WILLOUGHBY: "Investigation of Particle Growth and Ballistic Effects on Solid-Propellant Rockets; UTC-2128-FR; 15 June 1966; AD-486262; (U).

(13) J. K. BURCHARD and P. G. WILLOUGHBY: "Investigation of Performance Losses and Ballistic Effects in Solid-Propellant Rockets"; UTC-2197-FR; 14 April 1967; AD-815115; (U).

(14) P. G. WILLOUGHBY: "Investigation of Internal Ballistic Effects in Spinning Rocket Motors"; UTC-2281-FR; June 1968; (U).

(15) E. J. STURM: "A Study of the Burning Rates of Composite Solid Propellants in Acceleration Fields"; Ph.D. Thesis for the U. S. Naval Postgraduate School; March 1968; (U).

(16) G. B. NORTHAM: "An Experimental Investigation of the Effects of Acceleration on the Combustion Characteristics of an Aluminized Composite Solid Propellant"; CPIA Publication No. 111, Volume II; July 1966; AD-373908; (U).

APPENDIX A

ACCELERATION DATA QUESTIONNAIRE

EMERSON ELECTRIC

COMPILATION OF SPIN DATA PROGRAM - Acceleration Data Questionnaire

THIS DATA SUBMITTED BY:

_____ _____ _____

name

_____ _____ _____

title

_____ _____ _____

mail station

_____ _____ _____

telephone ext.

_____

organization

_____

address

_____

city state zip

_____

area code telephone

For personal interview to discuss data submitted, please contact:

_____ _____

name telephone

EMERSON ELECTRIC

COMPILATION OF SPIN DATA PROGRAM - Acceleration Data Questionnaire

PART I - Reference Sources

Known sources of data on the behavior of solid propellants in acceleration fields (exclusive of those listed in Emerson Electric Report #2122-1):

COMPILATION OF SPIN DATA PROGRAM - Acceleration Data Questionnaire

PART II - Analytical Studies

Program Title:_____

Contract No.:_____

Contracting Agency (Contractor):_____

Report Number(s):_____

_____

Concurrent Experimental Program?_____ Yes_____ No

Summary of Results: _____

_____

_____

_____

_____

_____

_____

_____

_____

_____

_____

_____

_____

_____

Is this or a related effort currently in progress?_____Yes_____No

EMERSON ELECTRIC

COMPILATION OF SPIN DATA PROGRAM - Acceleration Data Questionnaire

PART III - Test Facilities

A) Spin Test Facilities

Cognizant director: _____

Program (Contract) under which constructed:

_____

Limitations: Please describe, including -

Maximum spin rate: _____ RPM

Maximum allowable motor diameter: _____ IN

Maximum allowable motor length: _____ IN

Maximum allowable motor mass: _____ LB_m

Maximum allowable motor thrust: _____ LB_f

Physical description:

Please describe, including photos, drawings, or sketches.

Driving power source: _____

Data acquisition equipment:

Please describe, indicating: (1) instrumentation used to measure, transmit, and record pressure/time, thrust/time, and spin rate data; (2) calibration standards and procedures.

Automatic data reduction equipment: please describe.

Motor conditioning facilities: please describe.

This facility would (not) be available for use under contract with NASA Langley Research Center by _____ (date).

Comments _____

_____

EMERSON ELECTRIC

COMPILATION OF SPIN DATA PROGRAM - Acceleration Data Questionnaire

B) Centrifuge Test Facilities

Cognizant director: _____

Program (Contract) under which constructed:

_____

Limitations: Please describe, including -

Maximum allowable motor diameter: _____ IN

Maximum allowable motor length: _____ IN

Maximum allowable motor mass: _____ LB_m

Maximum allowable thrust: _____ LB_f (0^o to arm)

_____ LB_f (90^o to arm)

Maximum acceleration: _____ g's at _____ RPM

Physical description:

Please describe, including photos, drawings, or sketches.

Multidirectional mounting capability: ____ Yes ____ No

Data acquisition equipment:

Please describe, indicating: (1) instrumentation used to measure, transmit, and record pressure/time, thrust/time, and acceleration data; (2) calibration standards and procedures.

Automatic data reduction equipment: please describe.

Motor conditioning facilities: please describe.

This facility would (not) be available for use under contract with NASA Langley Research Center by _____ (date).

Comments _____

_____

EMERSON ELECTRIC

COMPILATION OF SPIN DATA PROGRAM - Acceleration Data Questionnaire

PART IV - Motor Performance

Program Title: _____

Contract Number: _____

Contracting Agency or Contractor: _____

1. Propellant Data:

(a) Propellant Designation: _____

(b) Propellant Type: _____

(c) Propellant Composition (including particle sizes):

_____

_____

_____

_____

_____

_____

(d) Burning Rate Data: (Static)

1) Base Burning Rate: _____ IN/SEC at _____ PSIA

2) Burning Rate Exponent: _____

3) Temperature Coefficient: _____

4) Effects of Strain: _____

_____

(e) Flame Temperature _____ ^{o}R

COMPILATION OF SPIN DATA PROGRAM - Acceleration Data Questionnaire

(f) Ratio of Specific Heats: _____

(g) Characteristic Velocity: _____ FT/SEC

(h) Propellant Density: _____ LB/IN^3

(i) Exhaust Product Molecular Weight: _____

(j) Storage Characteristics Summary: _____

_____

(k) Structural Properties:

1) Relaxation Modulus as a Function of Reduced Time or Reduced Rate; Modified Power Law Fit: _____

_____

2) Temperature Shift Factor; WLF Equation Form:

_____

3) Smith Envelope of Uniaxial Data

4) Biaxial Strip Data; Maximum Stress, Strain at Maximum Stress vs. Temperature (Specify crosshead speed) or Reduced Time.

5) Linear Coefficient of Thermal Expansion _____ $IN/IN-^oF$

6) If Case Bonded, Stress Free Temperature _____ ^oF

7) Insulation/Inhibitor/Propellant Bond Strength _____ PSI

COMPILATION OF SPIN DATA PROGRAM - Acceleration Data Questionnaire

2. Grain Configuration:

(a) Engineering Drawing of Grain and Inhibitor

1) Geometric Dimensions

2) Surface Area vs. Web

3) Sliver Fraction: _____

(b) Summary of Processing (Non-Proprietary): _____

_____

_____

(c) Cure Temperature History: _____

_____

(d) Type of Bonding: _____

3. Igniter Characteristics:

(a) Drawing of Igniter

(b) Igniter Designation: _____

(c) Igniter Type: _____

(d) Weight of Charge: _____

(e) Initiator Type: _____

(f) Charge Characteristics: _____

_____

(g) Orientation and Location Relative to Grain: _____

_____

COMPILATION OF SPIN DATA PROGRAM - Acceleration Data Questionnaire

4. Motor Configuration (Assembly Drawing)

(a) Chamber Configuration

1) Nominal Case Dimensions

2) Case Material: _____

3) Insulation Material: _____

4) Insulation Dimensions

(b) Nozzle Configuration:

1) Throat Area _____ IN^2

2) Number of Nozzles _____

3) Expansion Ratio _____

4) Half Angle _____ Degrees

5) Cant Angle _____ Degrees

6) Baffle or Flow Straighteners (Description) _____

_____

5. Performance Data for Each Test:

(a) Data Summary on Following Page

(b) Pre-Test Acceleration History

(c) Spin Rate vs. Time

(d) Motor Chamber Pressure vs. Time

(e) Thrust vs. Time

(f) Results of Post-Test Inspection

1) Unburned Slivers or Residue

2) Char Pattern on Burned Insulation

3) Erosion Pattern on Nozzle

EMERSON ELECTRIC

COMPILATION OF SPIN DATA PROGRAM - Acceleration Data Questionnaire

PERFORMANCE DATA FOR (MOTOR IDENTIFICATION): _____

Serial No. of Motor					
Date of Firing					
Location of Test					
Conditioning Temperature (^{O}F.)					
Test Cell Pressure (PSIA)					
Initial Mass (Pounds)					
Final Mass (Pounds)					
Pre-Test Throat Area (IN^2)					
Post-Test Throat Area (IN^2)					
Burn Time* (Seconds)					
Action Time** (Seconds)					
Total Impulse over Burn Time (LB_f-SEC)					
Total Impulse over Action Time (LB_f-SEC)					
Pressure Integral over Burn Time (PSIA-SEC)					
Pressure Integral over Action Time (PSIA-SEC)					

* Burn time is defined as _____

_____

** Action time is defined as _____

_____

APPENDIX B

DATA SOURCES

DATA SOURCES

Aerojet General Corporation
Sacremento, California 75814
(916-355-1000)
- L. Stone

Aerospace Corporation
111 E. Mill Street
San Bernardino, California 92408
(714-884-9211)
- A. Garthenburg
- A. Mager

Arnold Engineering Development Center
Air Force Systems Command
Arnold Air Force Station, Tennessee 37389
(615-455-2611)
- Lt. Col. J. R. Henry

Atlantic Research Corporation
Shirley Highway at Edsall Road
Alexandria, Virginia 22309
(703-354-3400)
- M. K. King
- B. F. Rohrbach

Auburn University
Auburn, Alabama 36830
(205-887-6511)
- R. H. Sforzini

AVCO Corporation
Ordnance Division
Sheridan Street
Richmond, Indiana 47374
(317-962-5511)
- R. E. Dekoltz

Ballistics Research Laboratory
Terminal Ballistics Laboratory
Aberdeen Proving Ground, Maryland 21005
(301-278-5201)
- E. L. Bannister
- A. Thrailkill

DATA SOURCES

Budd Company
Philadelphia, Pennsylvania 19105
(215-225-9100)
- R. H. Marvin

Cummins Engine Co., Inc.
1000 Fifth St.
Columbus, Indiana 47201
(812-372-7211)
- R. L. Glick (607)

Douglas Aircraft Corporation
Missile and Space Systems Division
2000 Ocean Park Blvd.
Santa Monica, California 90405
- T. J. Schweitzer (7438)

Fluidyne Engineering Corp.
5900 Olson Highway
Minneapolis, Minnesota
(612-544-2721)
- J. S. Holdhusen

Fluidyne Engineering Corp.
Suite 203
1000 E. Apache Blvd.
Tempe, Arizona 85281
(602-966-0232)
- G. H. Nelson

Hercules Powder Company
Allegany Ballistics Laboratory
P.O. Box 210
Cumberland, Maryland 21501
(304-726-4500)
- K. B. Kramer

Illinois Institute of Technology
Research Institute
Chicago, Illinois 60616
(312-225-9600)
- J. Pinsky

DATA SOURCES

Jet Propulsion Laboratory
California Institute of Technology
4800 Oak Grove Dr.
Pasadena, California 91103
(213-354-3108)
- P. F. Massier
- L. Strand

Ling-Temco-Vought
Vought Aeronautics Division
Dallas, Texas 75222
(214-262-3211)
- D. E. Lee
- S. Tolbert

A. D. Little, Inc.
Acorn Park
Cambridge, Massachusetts 02140
(617-864-5770)
- E. K. Bastress

Lockheed Missiles and Space Corp.
P.O. Box 504
Sunnyvale, California
- C. Bernard

Lockheed Propulsion Co.
Redlands, California 93274
(714-793-2211)
- D. E. Cantey

Naval Missile Center
P.O. Box 15
U.S. Naval Station
Point Mugu, California 93041
(805-488-3511)
- D. Stork (8184/7033)

Naval Ordnance Laboratory
White Oak
Silver Spring, Maryland 20910
(301-495-8153)
- C. Boyars

DATA SOURCES

Naval Ordnance Test Station
China Lake, California 93557
(714-377-7411)
- R. B. Dillinger (9374/9328)
- R. Feist (9217/9394)

Naval Postgraduate School
Monterey, California 93940
(408-372-7171)
- E. J. Sturm

Naval Weapons Laboratory
Dahlgren, Virginia 22448
(703-633-2511)
- R. B. Butler

Nortronics
500 E. Orangethorpe
Anaheim, California 92805
(714-871-5000)
- V. Peak (617)

U.S. Army Munitions Command
Picatinny Arsenal
Dover, New Jersey 07801
(201-328-4021)
- S. J. Harnett

Purdue University
Jet Propulsion Center
W. Lafayette, Indiana 47907
(317-734-9553)
- M. L'Ecuyer
- J. D. Hoffman

Redel, Inc.
2300 E. Katella Avenue
Anaheim, California 92805
(714-532-2586)
- J. W. DeDapper

DATA SOURCES

U.S. Army Missile Command
Propulsion Laboratory
Redstone Arsenal
Huntsville, Alabama 35809
(205-876-)
- W. D. Guthrie (-0441)

Rocketdyne
Solid Rocket Division
McGregor, Texas 76657
(817-475-2811)
- J. W. Wells (1669/1670)

Rohm and Haas Co.
Redstone Arsenal Research Division
Redstone Arsenal
Huntsville, Alabama 35809
(205-876-9811)
- L. J. Hurt
- C. Thies

Thiokol Chemical Corp.
Elkton Division
Elkton, Maryland 21921
(301-398-3000)
- W. G. Andrews (658)

Thiokol Chemical Corp.
Huntsville Division
Redstone Arsenal
Huntsville, Alabama
(205-876-)
- L. H. Caveny (-9558)
- B. K. Hodge

United Technology Corp.
1050 East Arques Avenue
Sunnyvale, California 94086
(408-739-4880)
- B. L. Iwanciow
- P. Willoughby

APPENDIX C

DATA REDUCTION AND NORMALIZATION COMPUTER PROGRAM

SECTION C-1

INTRODUCTION

The Data Reduction and Normalization (DRN) computer program was developed by the Emerson Electric Co. for the NASA Langley Research Center as part of the overall program task associated with the Compilation of Rocket Spin Data performed under Contract No. NAS1-6833. As described in Section III of this report, the DRN program not only accomplishes the usual objectives of integrating and averaging motor test data, but also compares the data thus obtained with two different methods of estimating the effects of acceleration environments on solid propellant burning rate. Using the FORTRAN IV computer language to allow maximum ease of engineering interpretation, this program was specifically written for the CDC 6400 digital computer system.

The data input parameters and format required are described in Section C-2, with a similar description of the output parameters provided in Section C-3. The complete program listing is included in Section C-4.

SECTION C-2

DATA INPUT

As indicated in Table C2-1, six (6) basic data input cards are required for each test firing. In addition, up to 30 pressure/thrust-time data points may also be included for each test. With the exception of the test identification number (card #1), the data input parameters are arranged in 14-digit fields. Although these fields need not be left- or right-adjusted, each must contain a decimal. Up to 70 alpha-numeric characterers may be included in the test identification number.

The limitation to a maximum of 30 pressure/thrust data points may be extended simply by revising the program DIMENSION statement to expand the data storage matrix. Thus the upper limit on the number of data points is a function only of computer storage capacity. A NASA Langley revision of this program currently allows up to 60 points.

Input Parameters

All data input parameters are defined below, along with the units required.

Card (1): Test firing identification number.

Card (2):

S = S_i = initial propellant surface area; IN^2

X0 = l_o = initial grain length; IN
= 0.0 for centrifuge slab tests

Y0 = r_i = inside radius of cylindrical grain; IN
= 0.0 for centrifuge slab tests

Y2 = r_o = outside radius of cylindrical grain; IN
= 0.0 for centrifuge slab tests

ENDS = E = number of (cylindrical) grain ends burning; -
= 0.0 for neutral-burning grain configuration

Card (3):

RX = r_x = (base) burn rate at reference pressure P_x; IN/SEC

EXP1 = n_1 = burn rate pressure exponent for P $\leq$ PEXP12; –

EXP2 = n_2 = burn rate pressure exponent for P > PEXP12; –

PX = P_x = reference pressure; PSIA

PEXP12 = pressure at n transition, if applicable; PSIA

Card (4):

CDTH = C_{Dt} = nominal mass flow coefficient; LB_m/LB_f-SEC

RHO = ϱ_t = nominal propellant density; LB_m/IN^3

A*I = A_{*i} = pre-test nozzle throat area; IN^2

A*F = A_{*f} = post-test nozzle throat area; IN^2

Card (5):

WEB = W = measured grain web thickness; IN

MEXP = m = mass of propellant expended; LB_m

GRAD = initial radius from motor centerline or centrifuge axis to the propellant surface; IN
= r_i for cylindrical motor spin tests

GEOM = 1.0 for neutral-burning grain geometries
= 0.0 for non-neutral grain geometries

PTS = number of input pressure/thrust-time data points (30.0 maximum)

Card (6):

RPM = spin rate of test motor or centrifuge; REV/MIN

TFINAL = t_f = final (return to 0 PSI) action time; SEC

TBURN = t_b = time to web burnout; SEC

TOL = % tolerance desired for surface area convergence (10^{-4}); –

Card (6): (cont'd)

MP = m_p = initial mass of propellant; LB_m
= mass expended (m) plus mass of residue

Cards 7-36:

T = t = time; SEC

PC = P = combustion pressure; PSIA

F = F = thrust; LB_f

TABLE C2-1: DRN Computer Program Data Input Format

1	IDENTIFICATION				70	71
						1

1 S 14	15 X0 28	29 Y0 42	43 Y2 56	57 ENDS 70	71
RX	EXP1	EXP2	PX	PEXP12	2
PI(π)	CDTH	RHO	A*I	A*F	3
3.1416					
WEB	MEXP	GRAD	GEOM	PTS	4
RPM	TFINAL	TBUFN	TOL	MP	5
					6

1 T 14	15 PC 28	29 F 42

1 T 14	15 PC 28	29 F 42

SECTION C-3

DATA OUTPUT

As indicated in the sample printout enclosed as Table C3-1, the DRN program calculates 47 motor performance parameters for each pressure/thrust-time data-input point. In addition, 11 parameters are provided at web burnout and 2 at final time.

For ready reference, each printout page is headed by the data input parameters and two reference quantities calculated for each motor firing:

PTH = P_t = the theoretical average motor operating pressure based upon the average propellant surface area and nozzle throat area; PSIA

TTH = t_t = the theoretical web burn time based upon P_t and the static (non-accelerating) burn rate/pressure relationship; SEC

Output Parameters

All data output parameters are defined below, along with the formulas used to calculate these quantities, where applicable.

Column	Quantity
1	TIME = t = (actual time) - (initial time); SEC
	A* = A_* = instantaneous nozzle throat area; IN^2
	$= A_{*i} + (A*_f - A*_i)(t/t_B) \exp (t/t_B - 1)$
	CF = C_F = thrust coefficient = F/PA_*; —
2	PC = P = measured combustion pressure; PSIA
	PTH = P_r = theoretical (instantaneous) combustion pressure based upon propellant surface area and no burn rate augmentation; PSIA
	$= P_x \left[\rho r_x (S_{Rr} + S_{er})/C_D P_x A_*\right]^{1/(1-n)}$
	PRAF = P_A = pressure at which motor would be operating with constant burn rate augmentation (AF); PSIA
	$= P_x \left\{\rho r_x [(AF) S_{RA} + S_{ea}]/C_D P_x A_*\right\}^{1/(1-n)}$

Column	Quantity
3	T/TBURN = t/t_B
	PC/PTH = P/P_r
	PC/PRAF = P/P_A
4	IPC = $\int_0^t P\,dt$; PSIA-SEC
	IPTH = $\int_0^t P_r\,dt$; PSIA-SEC
	IPRAF = $\int_0^t P_A\,dt$; PSIA-SEC
5	RTH = r_t = theoretical burn rate at P with no burn rate augmentation; IN/SEC
	= $r_x\ (P/P_x)^n$
	RAF = r_A = burn rate at P assuming constant burn rate augmentation; IN/SEC
	= $(AF)\,r_t$
	RATE = r_r = burn rate required to yield calculated mass flow rate; IN/SEC
	= $(\dot{m}_o - \dot{m}_{er})/\rho\, S_{Rr} = (C_D P A_* - \rho\, r_t S_{er})/\rho\, S_{Rr}$
6	RATE/RAF = r_r/r_a
	RATE/RTH = $r_r/r_t = (AF)\ (r_r/r_a)$
7	WTH = W_t = theoretical web consumed to time t with no burn rate augmentation; IN
	= $\int_0^t r_t\,dt$
	WRAF = W_A = web consumed to time t assuming constant burn rate augmentation; IN
	= $(AF)\ W_t$
	WRATE = W_r = web consumed to time t based upon r_r; IN
	= $\int_0^t r_r\,dt$

Column	Quantity
7	WRATE = $W_r = \int_o^t (\dot{m}_o W/m_p)\,dt = W(m_o/m_p)$ for CONSTANT SURFACE
8	WTH/WEB = W_t/W
	WRAF/WEB = $W_A/W = (AF)W_t/W$
	WRATE/WEB = W_r/W
	$= m_o/m_p$ for CONSTANT SURFACE
9	MDRAF/MDR = $\dot{m}_A/\dot{m}_r$
	$= (m_p/W)(r_A/\dot{m}_o)$ for CONSTANT SURFACE
	WRATE/WAF = $W_r/W_A = W_r/(AF)W_t$
	$= (m_o/m_p)[W/(AF)W_t]$ for CONSTANT SURFACE
	WRATE/WTH = $W_r/W_t = (AF)W_r/W_A$
	$\doteq (m_o/m_p)(W/W_t)$ for CONSTANT SURFACE
10	MDO = $\dot{m}_o$ = calculated nozzle efflux rate; LB_m/SEC
	$= C_D P A^*$
	MDRAF = $\dot{m}_A$ = mass generation rate from surface normal to acceleration vector assuming constant burn rate augmentation (method [A]); LB_m/SEC
	$= \rho S_{RA} r_A$
	$= (m_p/W) r_A$ for CONSTANT SURFACE
	MDE = $\dot{m}_{er}$ = mass generation rate from surface(s) parallel to the acceleration vector for method [B] ; LB_m/SEC
	$= \rho S_{er} r_t$
	$= 0$ for CONSTANT SURFACE
11	MDRATE = $\dot{m}_r$ = mass generation rate from surface normal to the acceleration vector for method [B]; LB_m/SEC

Column	Quantity
11	MDRATE = $\dot{m}_r = \dot{m}_o - \dot{m}_{er}$
	$= \dot{m}_o$ for CONSTANT SURFACE
	MDRAF/MDO = $\dot{m}_A/\dot{m}_o$
	$= [(AF) r_{xmp}/C_D P_x A_* W] (P_x/P)^{1-n}$ for CONSTANT SURFACE
	MDE/MDO = $\dot{m}_{er}/\dot{m}_o$
	$= 0$ for CONSTANT SURFACE
12	$M_o = m_o$ = nozzle efflux integrated to time t; LB_m
	MA = $m_A = \int_o^t \rho S_{RA} (AF) r_t dt$
	$= (AF) m_p W_t/W$ for CONSTANT SURFACE
	$= m_p$ at (CONSTANT-SURFACE) BURNOUT (t_B)
	ME = $m_{er} = \int_o^t \rho S_{er} r_t dt$
13	MRATE/MRAF = m_r/m_A
	$= (W/W_A)(m_o/m_p)$ for CONSTANT SURFACE
	$= m_o/m_p$ at (CONSTANT-SURFACE) BURNOUT (t_B)
	MRAF/MO = m_A/m_o
	$= (W_A/W)\ (m_p/m_o)$ for CONSTANT SURFACE
	$= m_p/m_o$ at (CONSTANT-SURFACE) BURNOUT (t_B)
	ME/MO = $m_{er}/m_o = 1.0 - m_r/m_o$
14	MO/MEXP = m_o/m
	MRAF/MEXP = m_A/m
	$= (W_A/W)(m_p/m)$ for CONSTANT SURFACE
	$= m_p/m$ at (CONSTANT-SURFACE) BURNOUT (t_B)
	ME/MEXP = m_{er}/m

Column	Quantity
15	MRATE = $m_r = \int_o^t (\dot{m}_o - \dot{m}_{er})dt$
	$= m_o$ <u>for CONSTANT SURFACE</u>
	G = instantaneous acceleration level at the propellant surface; G's
	S = S_{Rr} = propellant surface area normal to the acceleration vector for method [B] ; IN^2
16	F = F = measured thrust; LB_f
	ISP = I_s = specific impulse; LB_f-SEC/LB_m
	$= F/\dot{m}_o$
	MRATE/MEXP = m_r/m

<u>AT BURNOUT</u> (t_B)

Average burn rate = W/t_B; IN/SEC

Average pressure = $[\int_o^{t_B} Pdt]/t_B = (IPC)/t_B = \bar{P}$

Average augmented rate pressure = $(IPRAF)/t_B = \bar{P}_A$

PRAFBAR/PCBAR = $\bar{P}_A/\bar{P}_C$ = (IPRAF)/(IPC)

Burning rate augmentation factor = (AF) = W/W_t

Average acceleration level = $[\int_o^{t_B} Gdt]/t_B = \bar{G}$

PCACC = $(\bar{P})(\bar{G})$

Average theoretical pressure = $[\int_o^{t_B} P_r dt]/t_B = (IPTH)/t_B = \bar{P}_r$

PTHBAR/PCBAR = $\bar{P}_r/\bar{P}$ = (IPTH)/(IPC)

PCBARN*N = $(\bar{P})^n$

Density correction factor = ρ/ρ_t

$= m_p/WS\rho_t$ <u>for CONSTANT SURFACE</u>

$= m_p/\pi\, l_o(r_o^2 - r_i^2)\rho_t$ <u>for CYLINDRICAL GRAINS</u>

AT FINAL TIME (t_F)

Average pressure = $(IPC)/t_F$

Discharge coefficient correction factor = C_D/C_{Dt}

$$= m/C_{Dt} \int_0^{t_F} PA_* dt$$

TABLE C3-1: Sample DRN Computer Program Output

```
        LANGLEY SLAB MOTOR     HDD PROPELLANT     MOTOR 1024     200 G                                    PAGE  4

          S= 24.00     X0=  0.00     Y0= 0.000     Y2= 0.000     ENDS=   0

   RX   EXP1 EXP2   PX   PTH     TTH      CUTH      RHO      A*I      A*F      WFB      GRAD   GEOM  PTS   RPM    TFINAL  TBURN   MEXP      M
 .207  .450 .600    603   240  3.3315  .00669   .0579    .1001    .1001    .4960   48.000     1    30   383.2    1.872  1.142   .684    .684

   TIME      PC      T/TBURN     IPC       WTH                    WTH      WTH/WEB   MDRAF/MDR  MDO      MDRATE          MO     MRATE/MRAF  MO/MEXP  MRATE      F
    A*       PTH     PC/PTH      IPTH      WRAF     RATE/WAF      WRAF     WRAF/WEB  WRATE/WAF  MDRAF    MDRAF/MDO       MRAF   MRAF/MO     MRAF/MEXP  G          ISP
    CF       PRAF    PC/PRAF     IPRAF     WATE     RATE/RTH      WRATE    WRATE/WEB WRATE/WTH  MDE      MDE/MDO         ME     ME/MO       ME/MEXP    S          MRATE/MEXP

  1.0520     865     .9212       696     .2570                    .2295     .4627     1.1380     .6121     .6121          .4927     .7881     .7207     .493      -0.0000
   .1001     290    2.9828       305     .5054     .8788          .4513     .9099     .7921      .6966     1.1380         .6252     1.2689    .9145     201.422    0.0000
  0.0000    1195     .7239      1255     .4441    1.7281          .3575     .7207    1.5576     0.0000    0.0000         0.0000    0.0000    0.0000    24.000      .7207

  1.1420     815    1.0000       772     .2480                    .2522     .5085     1.1654     .5767     .5767          .5462     .7953     .7989     .546      -0.0000
   .1001     290    2.8103       331     .4870     .8581          .4960    1.0000     .7989      .6721     1.1654         .6868     1.2574    1.0046    201.583    0.0000
  0.0000    1195     .6820      1363     .4184    1.6874          .3963     .7989    1.5711     0.0000    0.0000         0.0000    0.0000    0.0000    24.000      .7989

 WEB BURNOUT HAS OCCURRED (TIME ABOVE)
                    AVERAGE BURN RATE =  .4343                    PCACC =   135787
                    AVERAGE PRESSURE =    676                     AVERAGE THEORETICAL PRESSURE =    267
                    AVERAGE AUGMENTED RATE PRESSURE =   1099      PTHBAR/PCBAR =  .3949
                    PRAFBAR/PCBAR=  1.6270                        PCBARN**N=  49.87
                    BURNING RATE AUGMENTATION FACTOR = 1.9665     DENSITY CORRECTION FACTOR =  .9920
                    AVERAGE ACCELERATION LEVEL = 200.97

  1.2120     745    1.0613       826     .2349                    .2691     .5426     1.2081     .5272     .5272          .5849     .7983     .8555     .585      -0.0000
   .1001     290    2.5689       351     .4620     .8278          .5292    1.0670     .8017      .6369     1.2081         .7326     1.2527    1.0716    201.700    0.0000
  0.0000    1195     .6234      1447     .3825    1.6278          .4243     .8555    1.5766     0.0000    0.0000         0.0000    0.0000    0.0000    24.000      .8555

  1.2720     615    1.1138       867     .2094                    .2825     .5695     1.3044     .4352     .4352          .6137     .7983     .8977     .614      -0.0000
   .1001     290    2.1204       368     .4118     .7666          .5555    1.1199     .8016      .5676     1.3044         .7688     1.2526    1.1244    201.787    0.0000
  0.0000    1195     .5146      1518     .3157    1.5076          .4453     .8977    1.5763     0.0000    0.0000         0.0000    0.0000    0.0000    24.000      .8977

  1.4520     215    1.2715       942     .1301                    .3137     .6326     2.3196     .1520     .1520          .6666     .7828     .9750     .667      -0.0000
   .1001     290     .7406       421     .2558     .4311          .6170    1.2439     .7838      .3526     2.3196         .8516     1.2775    1.2456    201.947    0.0000
  0.0000    1195     .1797      1733     .1103     .8478          .4836     .9750    1.5413     0.0000    0.0000         0.0000    0.0000    0.0000    24.000      .9750

  1.5120     115    1.3240       952     .0981                    .3206     .6465     3.2747     .0812     .0812          .6736     .7701     .9852     .674      -0.0000
   .1001     290     .3957       438     .1929     .3054          .6306    1.2713     .7750      .2659     3.2747         .8701     1.2918    1.2727    201.968    0.0000
  0.0000    1195     .0960      1805     .0589     .6005          .4887     .9852    1.5240     0.0000    0.0000         0.0000    0.0000    0.0000    24.000      .9852

  1.5720      65    1.3765       957     .0758                    .3254     .6571     4.4867     .0458     .0458          .6774     .7660     .9908     .677      -0.0000
   .1001     290     .2232       455     .1491     .2229          .6409    1.2921     .7668      .2055     4.4867         .8843     1.3054    1.2934    201.979    0.0000
  0.0000    1195     .0542      1877     .0336     .4383          .4914     .9908    1.5079     0.0000    0.0000         0.0000    0.0000    0.0000    24.000      .9908
```

SECTION C-4

DRN COMPUTER PROGRAM LISTING

```
                PROGRAM REDJM(INPUT,OUTPUT,TAPE2=INPUT,TAPE3=OUTPUT)
      C         REDUCTION OF ROCKET MOTOR PERFORMANCE DATA FOR CSD PROGRAM
      C         THIS PROGRAM WAS DEVELOPED BY EMERSON ELECTRIC CO. OF ST. LOUIS
      C         UNDER CONTRACT NO.  NAS1-6833          FEBRUARY 1968
000003           INTEGER CASE,PAGE, PASS
000003           REAL ISP, MDOUT, MDOTE, MDRAF, MOUT, MINE,
                1      MEXP, INTF, INTFF, KRPM2, MRAF, IPC, IPRAF,
                2      IPTH, MRATE, MDRAT1, MDRAT2, MRAT1, MRAT2,
                3      MRAT3, MRAT4, MRAT5, MRAT6, MRAT7, MDRATE,MDRATO,
                4 M
000003           DIMENSION T(30), PC(30), F(30), ASTAR(30), RTH(30),
                1          IPC(30), MDRAF(30), WRTH(30), RAF(30), MDOUT(30),
                2          ISP(30), MDOTE(30), MDRATE(30), RATE(30), PTH(30),
                3               PRAF(30), IDENT(7), MOUT(30), WRATE(30)
000003           INTF(DX, YJ, YK)=DX*(YJ+YK)*0.5
      C          READ THE TOTAL NUMBER OF CASES TO BE RUN IN THIS SERIES
      C          THIS DATA MUST APPEAR IN COLUMNS 1 AND 2 AND MUST BE RIGHT ADJUSTED
000013           READ (2, 2003) NCASE
000021           CASE=1
      C          READ IN DATA FOR ONE CASE (DATA MUST BE IN FIELDS OF 14 AND
      C          MUST CONTAIN A DECIMAL POINT IN EACH FIELD
000022    160    READ (2, 2000) (IDENT(I), I=1,7)
000034           READ (2,2001) S, X0, Y0, Y2, ENDS
000052           READ (2, 2001) RX, EXP1, EXP2, PX, PEXP12,
                1               PT, CDTH, RHOTH, ASTAR1, ASTARF,
                2               WEB, MEXP, GRAD, GEOM, PTS,
                3               RPM, TFINAL, TBURN, TOL, M
000126           PI = 3.1415926
```

```
000130          E = 2.71828
000131          NGEOM=GEOM
000133          NPTS=PTS
000134          CO=CDTH
000136          KRPM2=2.537E-5*RPM*RPM
000140          READ (2,2002) (T(I), PC(I), F(I), I=1, NPTS)
000156          TINIT = T(1)
000160          TBURN = TBURN - TINIT
000161          TFINAL = TFINAL - TINIT
000163          ABAR = ASTARI + (ASTARF - ASTARI)/E
000167          IF(NGEOM) 110, 110, 100
000170      100 SBAR = S
000172          RHO = M/(S*WEB)
000175          GO TO 120
000175      110 SBAR = PI*X0*(Y2+Y0)
000201          RHO = M/(PI*X0*(Y2*Y2-Y0*Y0))
000204      120 RHOCOR = RHO/RHOTH
000206          AF=1.0
000210          J=1
000211          IPC(J)=0.0
000212          WRTH(J)=0.0
000213          MOUT(J) = 0.0

            C       CALCULATE PARAMETERS WHICH WILL NOT CHANGE ON SECOND PASS

000214          DO 540 K=1, NPTS
000216          T(K) = T(K) - TINIT
000221          ASTAR(K)=ASTARI+(ASTARF-ASTARI)*(T(K)/TFINAL)
                1           *EXP(T(K)/TFINAL-1)
000237          IF(PC(K)-PEXP12) 450, 450, 470
000242      450 EXPON=EXP1
000244          GO TO 472
000244      470 EXPON=EXP2
000246      472 IF(PC(K) - 14.7) 474, 474, 480
000251      474 RTH(K) = 0.0
000253          GO TO 482
000253      480 RTH(K)=RX*(PC(K)/PX)**EXPON
000262       482 DT=T(K)-T(J)
```

```
000265          MDOUT(K)=CD*ASTAR(K)*PC(K)
000270          MOUT(K) = MOUT(J) + INTF(DT, MDOUT(J), MDOUT(K))
000277          IPC(K)=IPC(J)+INTF(DT, PC(J), PC(K))
000305          WRTH(K)=WRTH(J)+INTFF(DT, PC(J), PC(K), RTH(J),
                1         RTH(K), EXPON)
000315          J=K
000315          IF(T(K) - TBURN) 540, 490, 540
000317     490  WB = WRTH(K)
000321     540  CONTINUE
000324          AF=WEB/WB
000326          DISCOR=MEXP/MOUT(K)
000330          CD=CD*DISCOR
000331          PTH2 = PX*(RHO*RX*SBAR/(CD*PX*ABAR))**(1./(1.-EXP1))
000344          TTH = WEB/(PTH2/PX)**EXP1/RX
000352          IF(PTH2-PEXP12) 550, 550, 545
000354     545  PTH2 = PX*(RHO*RX*SBAR/(CD*PX*ABAR))**(1./(1.-EXP2))
000367          TTH = WEB/(PTH2/PX)**EXP2/RX

                C       CALCULATE PARAMETERS WHICH WILL CHANGE ON SUCCESSIVE PASSES

000375     550  WRAF=0.0
000376          MRAF=0.0
000377          MRATE=0.0
000400          MINE=0.0
000401          IPTH=0.0
000402          IPRAF=0.0
000403          PCONST=RHO*RX/(CD*PX)
000406          LINE = 0
000407          PAGE = 1
000410          J=1
000411          K=1
000412          RATE(1) = TOL
000414          WRATE(1) = 0.0
000415     600  DT=T(K)-T(J)
000420          IF(DT) 625, 625, 630
000422     625  DT = TOL
000424     630  I = 0
000425          IF(PC(K)-PEXP12) 640, 640, 660
000430     640  EXPON=EXP1
000432          GO TO 670
000432     660  EXPON=EXP2
000434     670  RAF(K)=RTH(K)*AF
000437          WRAF=WRTH(K)*AF
```

```
000440          MDOUT(K) = CO*ASTAR(K)*PC(K)
000443          MOUT(K) = MOUT(J) + TNTF(DT, MDOUT(K), MDOUT(J))
000452          IF(MOD(LINE, 7)) 680, 680, 690
000456      680 WRITE(3, 3000) (IDENT(I), I = 1, 7), PAGE,
               1       S, X0, Y0, Y2, ENDS
000504          WRITE(3, 3001) RX, EXP1, EXP2, PX, PTH2,
               1                TTH,CDTH, RHOTH, ASTAR1, ASTARF,
               2                WEB, GRAD, NGEOM, NPTS,
               3                RPM, TFINAL, TBURN, MEXP, M
000556          WRITE(3, 3010)
000562          PAGE = PAGE + 1

          C       CHECK THE GEOMETRY OF THE MOTOR

          C       FOR A CONSTANT SURFACE AREA, THIS NO. MUST BE 1--FOR A CYL. PORT

          C       WITH UNINHIBITED ENDS THIS NO. MUST BE 0.

000564      690 IF(NGEOM) 700, 700, 730
000566      700 X = X0 - ENDS*WRTH(K)
000572          Y = Y0 + WRATE(J) + RATE(J)*(T(K) -T(J))
000577          S = 2.*PI*X*Y
000603          SRAF = X*2.*PI*(Y0+WRAF)
000607          MDRAF(K) = RHO*SRAF*RAF(K)
000612      710 MDOTE(K) = ENDS*RHO*PTH(K)*PI*(Y2*Y2 - Y*Y)
000622           RATE(K) = (MDOUT(K)-MDOTE(K))/(RHO*S)
000627          IF(MDOTE(K) - MDOUT(K)) 702, 701, 701
000632      701 RATE(K) = 0.0
000634      702 WRATE(K) = WRATE(J) + TNTF(DT, RATE(J), RATE(K))
000643          Y = Y0 +*RATE(K)
000645          S2 = 2.*PI*X*Y
000650          SE = PI*(Y2*Y2-Y*Y)*ENDS
000654          I = I + 1
000655          IF(I-20) 711, 711, 998
000657      711 IF(ABS(S2/S-1.0)-TOL) 740, 712, 712
000664      712 S = S2
000666          GO TO 710
000666      730 MDOTE(K) = 0.0
000670          SE = 0.0
000671          RATE(K) = MDOUT(K)/(RHO*S)
000674          WRATE(K) = WRATE(J) + TNTF(DT, RATE(J), RATE(K))
```

```
000702          MDRAF(K) = RHO*S*RAF(K)
000705    740   MDRATE(K) = MDOUT(K)-MDOTE(K)
000710          MRAF=MRAF+INTF(DT, MDRAF(J), MDRAF(K))
000715          MINE=MINE+INTF(DT, MDOTE(J), MDOTE(K))
000722          MRATE = MOUT(K) - MINE
000724          TRAT=T(K)/TBURN
000726          WRAT1=WRTH(K)/WEB
000730          WRAT2=AF*WRAT1
000732          WRAT3 = WRATE(K)/WEB
000733          MRAT4 = MOUT(K)/MEXP
000735          MRAT5=MRAF/MEXP
000737          MRAT6=MINE/MEXP
000740          MRAT7=MRATE/MEXP
000742          GRAD2 = GRAD +WRATE(K)
000744          GLEVEL=GRAD2*KRPM2

                C       CHECK TO ASSURE THAT DENOMINATORS FOR RATIOS WILL NOT BE ZERO

000746          IF(PC(K) - 14.7) 790, 790, 800
000750    790   ISP(K) = 1.0
000752          CF = 1.0
000753          PTH(K) = 1.0
000754          PRAF(K) = 1.0
000755          MDRAT0 = 1.0
000756          MDRAT1 = 1.0
000757          MDRAT2 = 1.0
000760          RRAT2 = 1.0
000761          GO TO 810
000761    800   ISP(K) = F(K)/MDOUT(K)
000764          CF=ISP(K)*C0
000766          IF(PCONST*(S + SE)/ASTAR(K)-1.0) 801,802,802
000773    801   XPON = EXP1
000775          GO TO 803
000775    802   XPON = EXP2
000777    803   PTH(K) = PX*((PCONST*(S+SE)/ASTAR(K)))**(1./(1.-XPON))
001012          IF(PCONST*(S*AF+SE)/ASTAR(K)-1.0)804,805,805
001021    804   XPON = EXP1
001023          GO TO 806
001023    805   XPON = EXP2
001025    806   PRAF(K) = PX*((PCONST*(S*AF+SE)/ASTAR(K)))**(1./(1.-XPON))
```

```
001041          MDRAT0 = MDRAF(K)/MDRATE(K)
001043          MDRAT1=MDRAF(K)/MDOUT(K)
001045          MDRAT2=MDOTE(K)/MDOUT(K)
001047          RRAT2=RATE(K)/RAF(K)
001051      810 IF(K-1) 835, 835, 840
001054      835 WRAT5 = 1.0
001056          WRAT6 = 1.0
001057          MRAT1 = 1.0
001060          MRAT2 = 1.0
001061          MRAT3 = 1.0
001062          GO TO 860
001062      840 WRAT5 = WRATE(K)/WRAF
001065          WRAT6 = WRAT5*AF
001067          MRAT1=MRATE/MRAF
001071          MRAT2=MRAF/MOUT(K)
001073          MRAT3=MINE/MOUT(K)
001075          PCBAR = IPC(K)/T(K)
001077          PTHBAR = IPTH/T(K)
001101          PRAFB = IPRAF/T(K)
001103          PRRAT2=PTHBAR/PCBAR
001105          PBRAT3=PRAFB/PCBAR
001106      860 RRAT3=RRAT2*AF
001110          PCRAT2=PC(K)/PTH(K)
001113          PCRAT3=PC(K)/PRAF(K)
001115          IF(PCBAR-PEXP12)862,862,864
001117      862 XPON=EXP1
001121          GO TO 866
001121      864 XPON=EXP2
001123      866 PCBARN=PCBAR**XPON
001127          IPTH=IPTH+INTF(DT, PTH(J), PTH(K))
001134          IPRAF=IPRAF+INTF(DT, PRAF(J), PRAF(K))
001141      870 WRITE(3, 3011)T(K),PC(K),TRAT,IPC(K),RTH(K),WRTH(K),WRAT1, MDRAT0,
                1                   MDOUT(K), MDRATE(K), MOUT(K), MRAT1, MRAT4, MRATE,
                2                   F(K), ASTAR(K), PTH(K), PCRAT2, IPTH,
                3                   RAF(K), RRAT2, WRAF, WRAT2, WRAT5,
                4                   MDRAF(K), MDRAT1, MRAF, MRAT2, MRAT5,
                5                   GLEVEL, ISP(K), CF, PRAF(K), PCRAT3, IPRAF,RATE(K),
                6                   RRAT3, WRATE(K), WRAT3, WRAT6, MDOTE(K), MDRAT2,
                7                   MINE, MRAT3, MRAT6, S, MRAT7
```

```
001303          LINE = LINE +1
001305          IF(T(K)-TBURN)940, 930, 940
001307     930  WRITE(3, 3020)
001313          GBAR = (GRAD +WEB*0.5)*KRPM2
001317          RBAR = WEB/TBURN
001321          PCACC = PCBAR*GBAR
001323          WRITE(3, 3019) RBAR, PCACC
001332          WRITE(3, 3021) PCBAR, PTHBAR, PRAFB, PBRAT2, PBRAT3,PCBARN
001352          WRITE(3, 3013) AF, RHOCOR, GBAR
001364     940  IF(T(K)-TFINAL)950, 980, 980
001367     950  J=K
001371          K=K+1
001372          GO TO 600
001373     980  WRITE(3, 3022)
001377          WRITE(3, 3012) PCBAR, DISCOR
001407     990  CASE=CASE+1
001411          IF(CASE-NCASE) 160, 160, 999
001414     998  WRITE(3,3098)
001420     999  STOP 77777
001422     2000 FORMAT(7A10)
001422     2001 FORMAT(5F14.4)
001422     2002 FORMAT(3(F14.4))
001422     2003 FORMAT(I2)
001422     3000 FORMAT(1H1, //// 9X, 7A10, 20X, 5H PAGE, I3, //
                1         10X, 4H  S=, F6.2, 7H    X0= F6.2,
                2 7H    Y0=, F6.3, 7H    Y2=, F6.3, 9H    ENDS=,F4.0//)
001422     3001 FORMAT(2X, 38H RX  EXP1 EXP2  PX  PTH    TTH    CDTH,
                1 3X,39H RHO    A*I    A*F   WEB    GRAD   GEOM ,
                2 40H  PTS   RPM   TFINAL  TBURN  MEXP     M  /
                3 1X, 3F5.3, 2F6.0, F7.4, F7.5, F6.4,2F7.4, F6.4,  F7.3, I4,
                4 I6, F9.1, F8.3, F7.3, F7.3, F7.3//)
001422     3010 FORMAT(2X, 11H TIME    PC, 12H   T/TBURN  , 12H IPC      RTH, 11X,
                1 26H WTH   WTH/WEB  MDRAF/MDR , 24H MDO    MDRATE       MO ,
                2 35H MRATE/MRAF  MO/MEXP  MRATE       F/
                3 3X, 45H A*    PTH   PC/PTH    IPTH    RAF  RATE/RAF ,
                4 51H WRAF  WRAF/WEB WRATE/WAF  MDRAF  MDRAF/MDO   MRAF ,
                5 35H MRAF/MO  MRAF/MEXP    G         ISP/
                6 3X,50H CF    PRAF  PC/PRAF   IPRAF  RATE  RATE/RTH WRATE,
                7 53H WRATE/WEB WRATE/WTH  MDE    MDE/MDO     ME     ME/MO,
                8 3X, 27H ME/MEXP     S   MRATE/MEXP//)
```

```
001422     3011 FORMAT(1X, F7.4, F7.0, F8.4, F8.0, F7.4, 8X, F8.4, F9.4, F9.4,
                1 5F9.4, F9.3, F10.4/
                2 2(1X, F7.4, F7.0, F8.4, F8.0, F7.4,2F8.4, 7F9.4, F9.3, F10.4/)/)
001422     3012 FORMAT(10X, 19H AVERAGE PRESSURE = , F7.0,
                1       10X,43H DISCHARGE COEFFICIENT CORRECTION FACTOR = ,F6.4)
001422     3013 FORMAT(20X, 36H BURNING RATE AUGMENTATION FACTOR = , F6.4,
                1 4X, 29H DENSITY CORRECTION FACTOR = ,  F6.4/
                2 20X,  29H AVERAGE ACCELERATION LEVEL =, F7.2/)
001422     3019 FORMAT(20X,21H AVERAGE BURN RATE = , F6.4, 13X, 9H PCACC = ,F8.0)
001422     3020 FORMAT(  38H WEB BURNOUT HAS OCCURRED (TIME ABOVE))
001422     3021 FORMAT( 20X, 19H AVERAGE PRESSURE =, F7.0,20X,
                1         31H AVERAGE THEORETICAL PRESSURE =, F7.0/ 20X,
                2         34H AVERAGE AUGMENTED RATE PRESSURE =,F7.0,5X,
                3         15H PTHBAR/PCBAR =,F7.4/ 20X,
                4         16H PRAFBAR/PCBAR= ,F7.4,23X,11H PCBARN**N=,F7.2)
001422     3022 FORMAT(11H FINAL TIME)
001422     3090 FORMAT(20X, I2,3(10X,E13.6))
001422     3098 FORMAT(///42H SURFACE AREA ITERATION FAILED TO CONVERGE)
001422          END
```

```
           REAL FUNCTION INTFF(DT, P1, P2, R1, R2, EXPON)

      C     FUNCTION SUBPROGRAM FOR CALCULATION OF INCREMENTAL INCREASES

      C     IN WEB BURNED

000007          IF(P1-P2)1,2,1
000011        1 INTFF = (P2*R2-P1*R1)*DT/((EXPON+1.)*(P2-P1))
000020          RETURN
000021        2 INTFF = R1*DT
000023          RETURN
000023          END
```